National Park Service
U.S. Department of the Interior

Natural Resource Stewardship and Science

Evaluation of Gully Erosion for Archaeological Preservation in Wupatki National Monument

Natural Resource Report NPS/WUPA/NRR—2024/2630

ON THE COVER
Cliffs of the Moenkopi Formation influence runoff processes and concentrate flow into an eroding cinder landscape in Wupatki National Monument.
COLORADO STATE UNIVERSITY / CELESTE WIETING

Evaluation of Gully Erosion for Archaeological Preservation in Wupatki National Monument

Natural Resource Report NPS/WUPA/NRR—2024/2630

Celeste Wieting, Sara Rathburn, John Kemper

Colorado State University
Fort Collins, Colorado

February 2024

U.S. Department of the Interior
National Park Service
Natural Resource Stewardship and Science
Fort Collins, Colorado

The National Park Service, Natural Resource Stewardship and Science office in Fort Collins, Colorado, publishes a range of reports that address natural resource topics. These reports are of interest and applicability to a broad audience in the National Park Service and others in natural resource management, including scientists, conservation and environmental constituencies, and the public.

The Natural Resource Report Series is used to disseminate comprehensive information and analysis about natural resources and related topics concerning lands managed by the National Park Service. The series supports the advancement of science, informed decision-making, and the achievement of the National Park Service mission. The series also provides a forum for presenting more lengthy results that may not be accepted by publications with page limitations.

All manuscripts in the series receive the appropriate level of peer review to ensure that the information is scientifically credible and technically accurate.

This report is available in digital format from the Natural Resource Publications Management website. If you have difficulty accessing information in this publication, particularly if using assistive technology, please email irma@nps.gov.

Please cite this publication as:

Wieting, C., S. Rathburn, and J. Kemper. 2024. Evaluation of gully erosion for archaeological preservation in Wupatki National Monument. Natural Resource Report NPS/WUPA/NRR—2024/2630. National Park Service, Fort Collins, Colorado. https://doi.org/10.36967/2302447

NPS 322/192780, February 2024

Contents

Contents (continued)

Page

Figures

Figures (continued)

Page

Tables

Page

Executive Summary

Wupatki National Monument contains an abundance of prehistoric and historic archaeological sites that are vulnerable to gully erosion from heavy sporadic rainstorms. Increased erosional risks are predicted as more extreme weather causes frequent or intense rainfall, flooding, and gullying. At Wupatki National Monument, gullies generally form on hillslopes within volcanic-derived cinders that are ubiquitous across the landscape and are unconsolidated, non-cohesive, highly mobile, and permeable. Lithological differences between volcanic cinders and underlying sedimentary rocks, and surface runoff influence the progression of gully erosion near archaeological sites. We assessed gullies based on changes in gully morphology and categorized archaeological sites based on vulnerability from erosion and runoff processes. We found that 35 measured gullies are actively eroding, with statistically significant changes in gully depth from 2016 to 2021. Up to 0.5 m of incision was documented over a five-year period. A structure from motion analysis at the hillslope scale confirmed gully morphological changes and supports the applicability of conducting similar analyses on a larger scale. More erosion occurred in gullies with catchments predominantly covered with cinders because of cinder mobility. We noted a weak relationship between gully catchment area and gully head slope, likely related to runoff processes from outcrops of resistant sedimentary rocks forming cliffs and characteristics of cinders that maximize infiltration and transport. Based on our assessment of gully morphologic change and substrate characteristics, 22 archaeological sites along Wupatki Wash were identified as having a high vulnerability to erosion, helping monument managers to prioritize their monitoring initiatives.

Acknowledgments

The authors express our gratitude to everyone who has contributed to this research project. First and foremost, we thank Lisa Leap for her invaluable contributions to the project. Lisa's support was instrumental in securing the funding needed to carry out this research, and she shared her time and expertise to provide feedback that enhanced the quality of our work. We are grateful for her support and dedication to this project. We thank NPS archaeologists Jonathan Hardes, Shayna Marks, and James Mariano for providing field support and information about archaeological sites while conducting field work, and Kerry Gaiz for supplying NPS spatial data. We appreciate the comments from five internal NPS reviewers that helped clarify this report.

Chapter 1. Introduction and Study Background

1.1 Introduction

Hillslope gullies are problematic for cultural sites located across the Southwest (e.g., Pederson et al., 2006) and around the world (e.g., Gouma et al., 2011), putting important cultural artifacts at risk of erosion. Factors that contribute to the formation and development of gullies include processes such as water erosion from overland flow. The geology and topography of the landscape, soil and vegetation cover, and local climate influence erosion. Sediment yields tend to be greatest in semi-arid environments where precipitation is sufficient to generate soils and drive erosion, but limits vegetation growth that stabilizes hillslopes (Langbein and Schumm, 1958). In these environments, in particular, where the disparity between driving forces (precipitation) and resisting forces (vegetation) is increasing due to global climate warming, increased erosional risks are predicted as more extreme weather causes frequent or intense rainfall, and flooding (IPCC, 2021). At Wupatki National Monument (WUPA) located in northern Arizona (Figure 1), heavy sporadic rainstorms in the past decade, lack of vegetation, and presence of unconsolidated volcanic-derived cinders exposes archaeological sites to erosion. Mean annual temperature (~15°C) at WUPA is expected to increase and could shift soil moisture and precipitation patterns (Andrews et al., 2019). Wind and water work in concert to shape the landscape by mobilizing and concentrating cinders in lower topographic areas, and then mobilizing them during rainstorms. At WUPA, lithological differences between volcanic cinders and underlying sedimentary rocks, and landscape processes such as surface runoff influence the progression of gullies at or near archaeological sites. This research was conducted to collect baseline geomorphological data and identify archaeological resources of highest vulnerability to landscape erosion from rainfall events. From this study, managers can prioritize long-term management actions needed to protect archaeological resources within WUPA.

1.2 Previous Research

A gully is a relatively deep, eroding channel that forms on valley sides and on valley floors where no well-defined channel previously existed (Schumm et al., 1984). Typically, gullies are narrow, steep-sided channels, usually formed by the erosion of water (Thwaites et al., 2021) from head cut retreat, steepening of the gully walls, and eventually enlargement and collapse (Higgins et al., 1990). Processes responsible for head cut retreat include sapping at the gully base (Emmett, 1968) and concentrated overland flow. Where gullies have been studied on cinder cones (Dóniz et al., 2011), gully formation is attributed to concentrated overland flow during rain events, but gullies in these settings may be initiated by mud and debris flows (Dóniz et al., 2011). In semi-arid climates, gully erosion generally results from overland flow following short, intense precipitation events, and is not typically influenced by piping or seepage (Petersen, 2003; (Pederson et al., 2006).

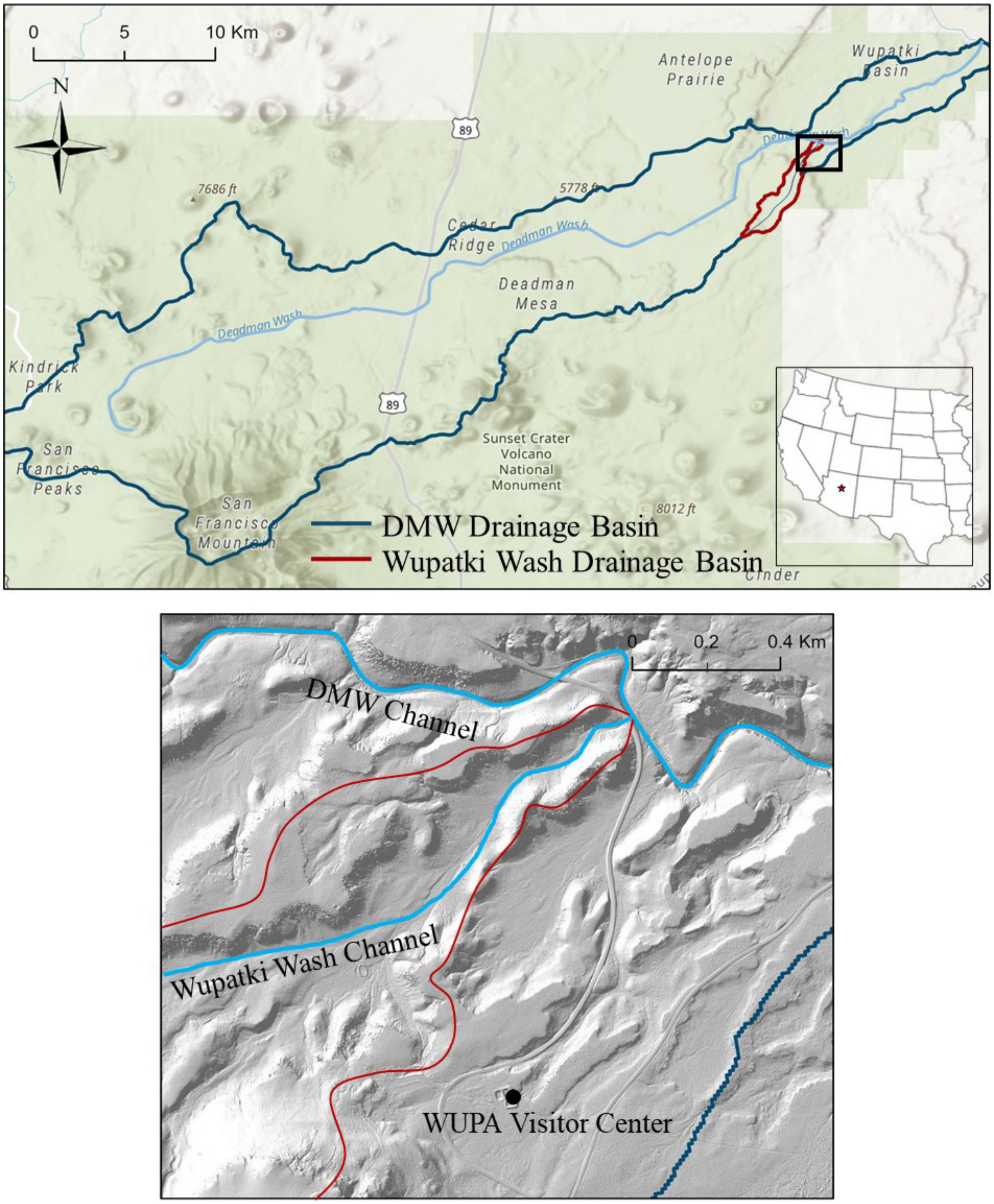

Figure 1. Drainage basin map of Deadman Wash (DMW) and Wupatki Wash. The callout box displays the confluence of the main Wupatki and Deadman Wash channels, near the WUPA Visitor Center.

Research into gully formation began with the recognition that considerable erosion resulted from the conversion from natural vegetative cover to crops, and the need for soil conservation practices, throughout the U.S (e.g., Ireland et al., 1939). Other research identified stages of gully development (Ireland et al., 1939; Bariss, 1972). Several studies have found a relationship between slope and contributing area that identifies a threshold for gully erosion (Patton and Schumm, 1975; Vandekerckhove et al., 2000; Wu and Cheng, 2005, Pederson et al., 2006). Patton and Schumm (1975) identified a geomorphic threshold valley slope for a given contributing area above which gullies formed in the Piceance Creek Basin, CO. Patton and Schumm (1975) found that the relationship between valley slope and contributing area did not pertain to drainage basins smaller than about 18 km^2 (1800 ha). In these small basins, variations in vegetative cover or variations in the properties of the alluvium prevented development of a critical threshold slope (Schumm et al., 1984). Pederson et al. (2006) also used the slope-area approach to identify threshold slopes and predict gully formation around archaeological sites in Grand Canyon. They identified gully erosion thresholds and found that gradient was the most important control on gully extent, but their topography-based predictive models lacked soil property influences and resulted in many false-positives. Our study fills a gap in knowledge of gully formation in small drainage basins (median=0.0285 ha; 285 m^2) where volcanic cinders cover underlying sandstone bedrock.

1.3 Study Objectives

To help WUPA managers prioritize long-term management actions to preserve the archaeological record, we evaluated the mechanisms that influence the evolution and expansion of gullies and assessed archaeological site vulnerability. We collected baseline geomorphological data at WUPA in summer 2021. To analyze hydrologic and erosional processes due to lithological differences, we quantified physical and hydraulic differences between Moenkopi- and cinder-dominated sediments. Additionally, we conducted a multiscale five-year geomorphic change analysis using aerial LiDAR (2016) and field-collected data (2021). The larger, coarse-scale analysis included 35 measured gullies across all of Wupatki Wash, while the high-resolution analysis was focused on a small hillslope in Wupatki Wash. Based on these analyses, we (1) assessed gullies based on changes in gully morphology, and (2) categorized archaeological sites within a small drainage with abundant archaeological sites based on vulnerability from erosion and runoff processes. We hypothesize that a threshold critical slope will be identified for a given contributing area above which gully erosion is expected. In addition, we hypothesize that lithology influences erosion such that Moenkopi-dominated catchments will increase runoff and show greater elevation change in gullies over time.

1.4 Study Area

Located about an hour's drive northeast of Flagstaff, Arizona, WUPA (Figure 1) is a culturally diverse area that contains over 2600 prehistoric and historic archaeological sites (Baldwin et al., 2015). Most sites are small one-room field houses with scattered artifacts, but the presence of large pueblos indicate prehistoric communities of people gathered in the WUPA area to trade, play, and reside (pers. comm., Lisa Leap).

1.4.1 Site Characteristics

There are three dominant geological materials found at WUPA: The Moenkopi Formation, the Kaibab Formation, and aeolian cinder deposits. The Moenkopi Formation consists of Triassic (~240 million years old) sandstones, siltstones and mudstones deposited in a variety of geologic settings including shallow marine, beach, tidal flat, lagoon, and floodplain (Billingsley et al., 2007). The term "Moenkopi-derived sediments" is used here to encompass the entire Moenkopi Formation, but generally refers to the sediments derived from sandstone members. The aeolian cinder deposits seen at WUPA are Quaternary in age and originated from Sunset Crater Volcano, located just south of WUPA. Sunset Crater Volcano erupted in 1085 AD, ejected basaltic volcanic fragments, and spread a layer of cinders on top of Moenkopi sedimentary rocks throughout WUPA (Hanson, 2003). Cinder deposits, originally deposited less than 10 cm thick (Hooten et al., 2001), then later redistributed by wind and water, acted as a mulch atop barren desert soils for prehistoric agricultural practices and helped increase infiltration and soil moisture, and decrease runoff (Grattan and Torrence, 2007). Aeolian transport of the cinders over time has created dune deposits throughout WUPA (Billingsley et al., 2007). Gullies and rills generally form within volcanic-derived cinders that blanket the Moenkopi Formation, or within Moenkopi sediments themselves. The Kaibab Formation also outcrops within WUPA, but cinder and Moenkopi-derived sediments are ubiquitous and more relevant in this study. We focus our analysis on the eastern portion of the monument, within Wupatki Wash, a tributary to Deadman Wash (Figure 1). The semi-arid study area hosts barren areas and sparsely vegetated sandstone outcrops and badlands (Hansen et al., 2004). Saltbrush (*Atriplex canescens*), Mormon tea (*Ephedra viridis*), Apache plume (*Fallugia paradoxa*), rabbitbrush (*Ericameria nauseosa*), and oneseed juniper (*Juniperus monosperma*) are common at WUPA (Hansen et al., 2004).

Wupatki Wash is an ephemeral channel that exhibits discontinuous flow during heavy rains due to the presence of permeable volcanic-derived cinders. WUPA receives an average annual rainfall of around 20 cm, most of which falls during the summer monsoon. Daily precipitation data were gathered from a weather station within WUPA (Station USC00029542) and analyzed to better understand the occurrence and intensity of rainstorms in the region. Several notable events took place in the summers of 2013, 2016, 2018, and 2022 (Figure 2). Additional higher temporal resolution (15 minute) precipitation data were received from National Park Service (NPS) staff for the month of August 2022. These data indicate that a 100-to-200-year precipitation event took place on August 15, 2022, when 4.24 centimeters of rain fell within 30 minutes (Figure 3). Short-duration, high intensity thunderstorms underscore the need to understand erosion and landscape change in semi-arid environments.

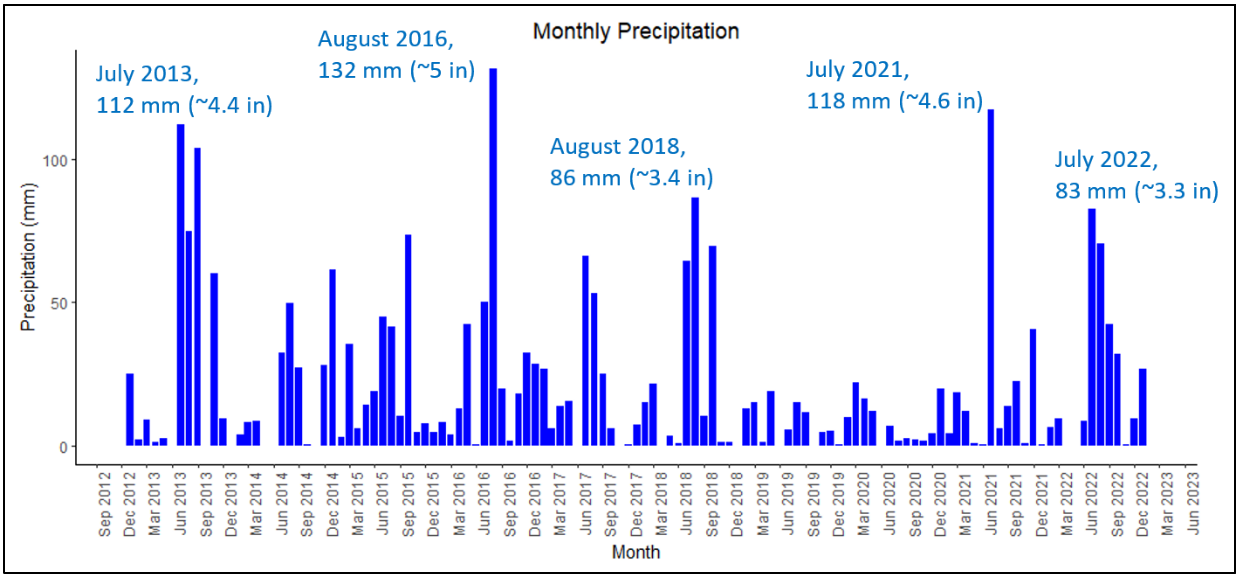

Figure 2. Monthly precipitation totals at WUPA, summarized from daily precipitation data. Daily precipitation and other weather data come from COOP station ID USC00029542, located within the monument.

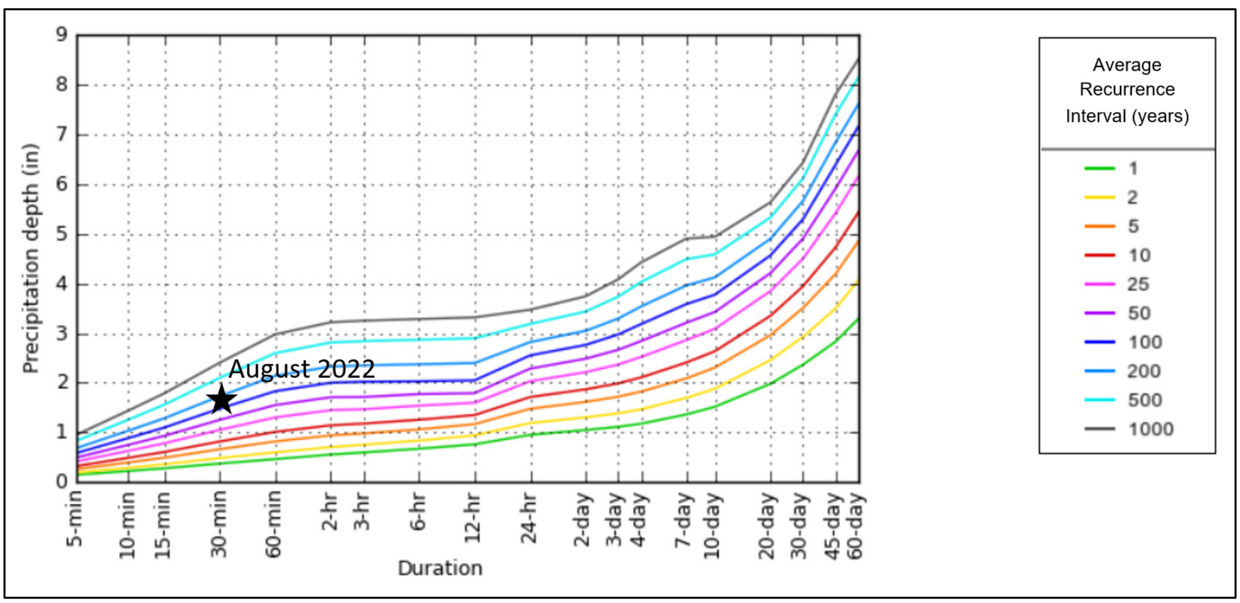

Figure 3. The August 15, 2022 rainstorm (1.67 inches in 30 minutes) is the equivalent to a 100- to 200-year precipitation event (NOAA, 2023).

At WUPA, water and sediment concentrate in concave regions of hillslopes due to surface flow off Moenkopi Formation sandstone that forms bands of cliffs (Figure 4). Cliff bands are laterally extensive conspicuous features with a near vertical slope (Figure 5). Incisional features found along cliff band convexities are generally parallel rills (smaller than gullies, no more than 0.3 m deep; Thwaites et al., 2020) formed within the Moenkopi Formation, due to the lack of accumulated cinder deposits. Gullies at WUPA generally originate at the vertical cliffs or rockfall area of Moenkopi sandstone, have a linear planform (Figure 5 and 6), are V-shaped in cross-section with banks and bed composed of primarily cinders, and have gradual, inclined gully heads (Thwaites et al., 2020). The elementary gully classification (EGC) was used to further classify gullies at WUPA (Figure 6) to help identify gully erosion processes.

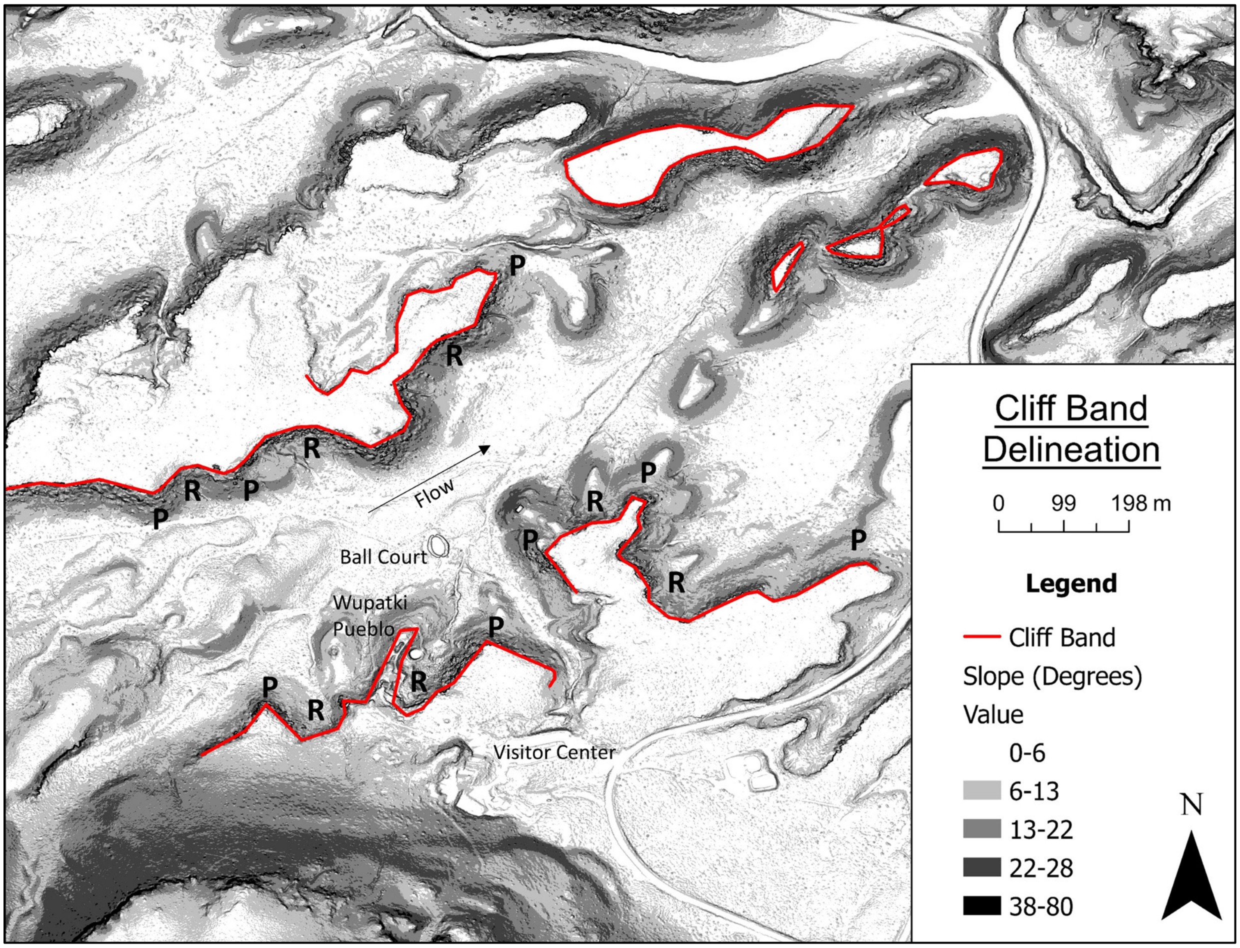

Figure 4. Map illustrating locations of points (P) and recesses (R) formed by linear cliff bands of Moenkopi Formation. Map adapted from Anderson (2021).

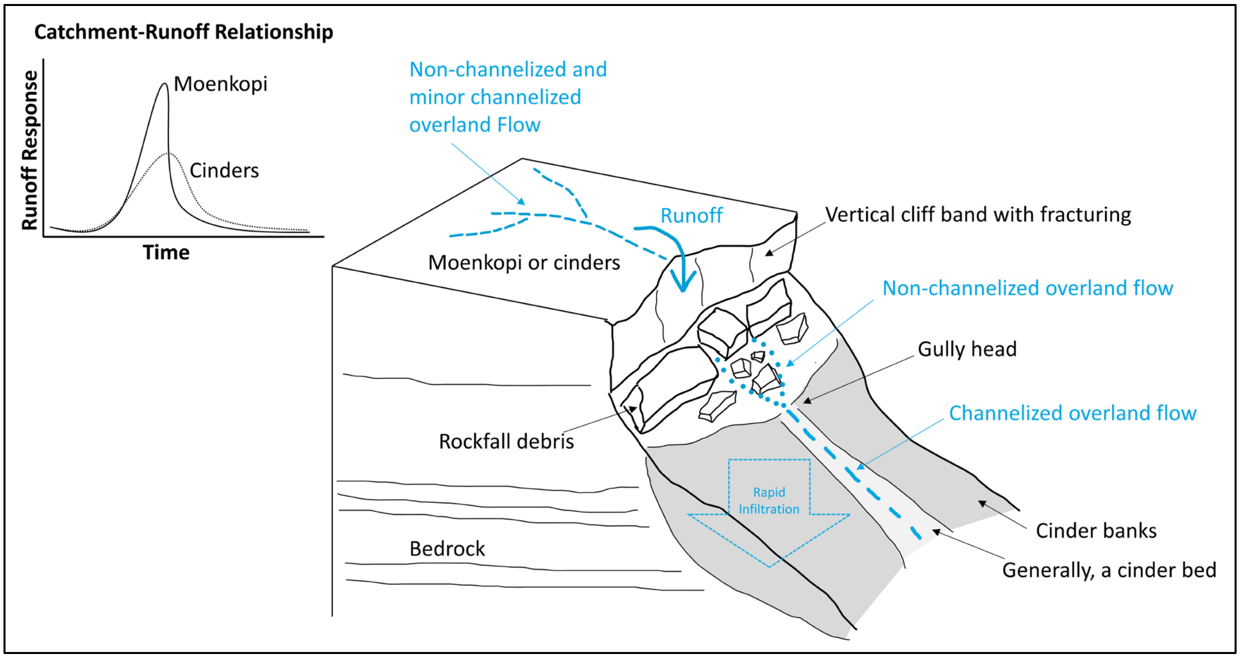

Figure 5. Conceptual diagram of the interaction between local geology and hydrological processes including infiltration, overland flow, and runoff. Following a rainstorm, water flows on the surface of catchments as either non-channelized or minor channelized overland flow, pours over cliff bands of Moenkopi sandstone, flows down hillslopes through rockfall, and eventually concentrates in gullies formed within cinder deposits on top of Moenkopi bedrock. Gully heads generally form near the base of rockfall material where channels initiated in cinder deposits. Depending on surface conditions in the gully catchment, we expect differences in the runoff response following a rainstorm (upper left graph): quicker, flashier runoff in catchments composed of predominantly Moenkopi sediments and bedrock compared to a more delayed and muted runoff response from catchments covered with cinders.

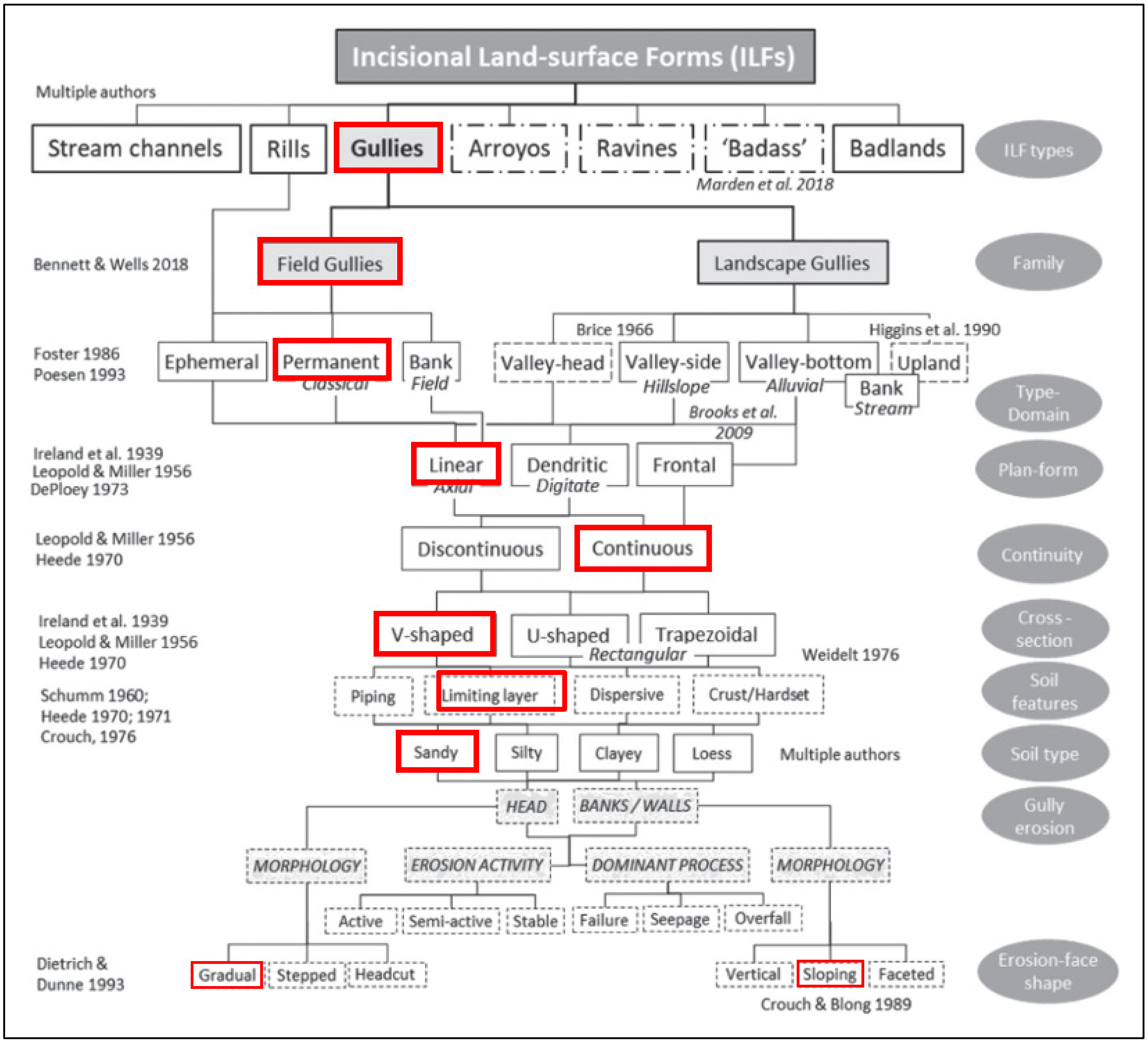

Figure 6. Classification of gullies at WUPA (red boxes) using the elementary gully classification proposed by Thwaites et al. (2021). Gully erosion classifications including "erosion activity" and "dominant process" were investigated within this study and thus not outlined.

Chapter 2. Study Methods

2.1 Baseline Geomorphological Data Collection

When intense rainstorms occur in a semi-arid environment such as WUPA, surface characteristics determine the amount of water that infiltrates or runs off. A Mini Disk tension infiltrometer was used to quantify infiltration and estimate field-saturated hydraulic conductivities (K_{fs}) of surficial sediments in catchment areas of 17 gullies in Wupatki Wash. The infiltrometer was chosen because it is compact and requires minimal water. Water immediately begins infiltrating into the soil at a rate determined by the hydraulic properties of the soil (Decagon Devices, 2014), and the water level on the device is recorded over time. The shortest infiltration experiment ran for 2 minutes, and experiments generally were conducted for a maximum of 10 minutes. Where possible, at least 15–20 mL of water was infiltrated during each measurement for adequate calculation of K_{fs} (Decagon Devices, 2014). K_{fs} was calculated from infiltration data and Van Genuchten parameters related to the soil type (Decagon Devices, 2014). To ensure good contact between the infiltrometer and the surface, loose litter was removed from the surface. An average value of K_{fs} was calculated from three measurements conducted in the upper, middle, and lower portion of the catchment. Sediment samples were collected at each gully bed and left/right banks, and then sieved in the laboratory using standard sieving practices (ASTM, 2018). Four sediment types were compared: volcanic-derived cinders, and Moenkopi-derived clay, silty clay, and sand.

Additionally, we collected field-based information on catchment properties (catchment area, vegetation cover, surficial materials, and presence of cliff bands) that influence surface processes to examine linkages between catchments and gullies. Our data collection also tested previously quantified relationships between catchment area and gully head slope to identify topographic thresholds that initiate erosion in gullies (Patton & Schumm, 1975; Pederson et al., 2006). Vegetation cover was recorded as a percentage from 0–100% and then classified as low (0–30%), medium (31–70%), and high (71–100%). Cliff band height was measured using a laser range finder.

2.2 Topographic Data Collection and Landscape Analyses

2.2.1 Topographic Data Collection

A total of 35 gullies were surveyed using a Top Con Real-Time-Kinetic (RTK) surveying system (Figure 7) with sub-centimeter accuracy. At each gully, topographic point data were collected starting at the top of the gully's drainage catchment, down the center of the catchment and gully, and at three representative cross-sections, recording notable slope breaks (Figure 8). The three cross-sections were strategically located near the top, middle, and bottom of the gully channel. Ten larger gullies required additional cross sections. Initially, field data were collected to develop a relationship between catchment area and gully head slope to quantify a topographic threshold at which erosion initiates.

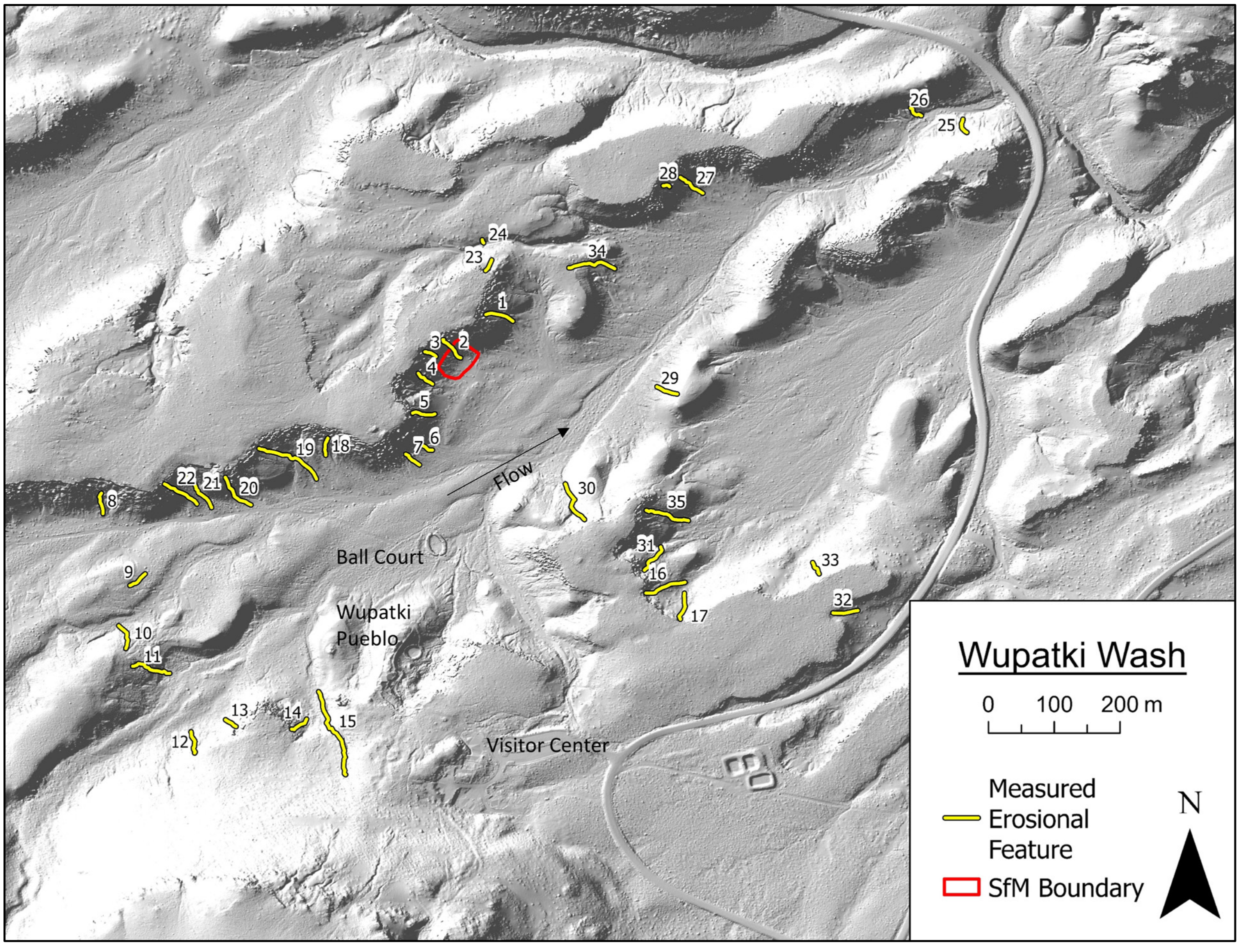

Figure 7. Map of the locations of 35 total gullies surveyed within WUPA and the boundary of the structure from motion (SfM) analysis.

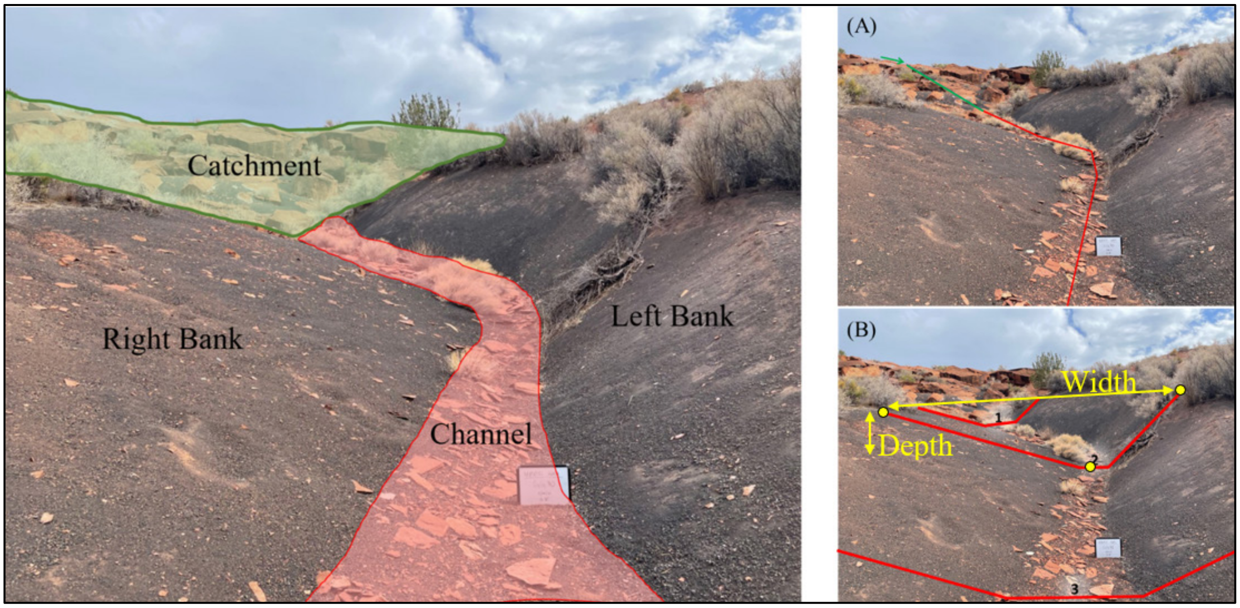

Figure 8. Example of topographic surveying methods used at each gully. (A) Surveys began at the top of the catchment, proceeded down the center of the catchment, and down the channel centerline. (B) Three cross-sections across the channel near the top, middle, and bottom of the gully were also surveyed. Yellow dots illustrate examples of points used for gully width and depth calculations for a single cross-section. For gully width, the top of bank locations was used and for gully depth, the vertical distance was calculated between the cross-section minimum elevation (bottom point) and lower of the two top bank elevations.

Longitudinal profiles were created in ArcGIS Pro (version 2.6.0) to compare field-collected (2021) to aerial LiDAR (2016) topographic data. Elevation data were extracted from elevation data collected from the 2016 LiDAR at the exact (x,y) coordinates from the 2021 surveyed point data using the "extract values to points" tool in ArcGIS Pro. Longitudinal profiles were used to calculate changes in gully head slope and median elevation difference (MED) over the five-year period, and cross-sections were used to calculate changes in gully dimensions including width, depth, and length. Gullies were then classified based on MED, and further evaluated for changes in width and depth individually. From cross-section data, top width was used for the average gully width, and the bottom to lowest top value was used for average gully depth (Figure 8). We analyzed whether statistical differences existed for average width and average depth changes using a paired nonparametric Wilcoxon signed rank test, with a significance level of 0.05. The gully head slope was identified as the region near the top of the gully channel where flow concentrates. Changes in gully head slope were used to describe changes to overall gully behavior.

2.2.2 Slope-Area Analysis and Gully Prediction

Similar to Pederson et al. (2006), we delineated a topographic threshold to predict gully erosion using gully head slope and catchment area:

$$S_c = aA^{-b}$$

Where S_c is the critical slope gradient (m/m), A is the catchment area (ha), a is a threshold coefficient and b is a scaling exponent. Catchment areas were delineated in the field with a handheld GPS, and then verified using WMS software (Aquaveo, 2022) due to difficulties distinguishing catchment boundaries in the field (low slope, homogenous surface material, and lack of channelized flow paths). Ultimately, for consistency, catchment areas obtained from WMS were used. Twenty-one of the 35 gullies were included in this analysis based on similarities in bed and bank materials, presence of a cliff band, and gully morphology. Gully head slope versus catchment area was plotted and fitted to a linear regression. The variables a and b were derived from a threshold line by shifting the regression line down to the base of the main scatter (Pederson et al., 2006).

The slope-area analysis to predict where gullies form was completed using ArcGIS Pro. First, the D∞ algorithm within the flow accumulation tool was used to create a contributing area raster (Tarboton, 1997). Then, two slope rasters were created: a threshold slope raster using the raster calculator tool and variables defined from the threshold line, and an "actual" slope raster generated from the 2016 aerial LiDAR. The gully prediction map was produced using the raster calculator tool by calculating where "actual" slope exceeds threshold slope.

2.2.3 Structure from Motion Analysis

For a high spatial resolution geomorphic change analysis and to evaluate topographic change over a five-year period, we applied the structure from motion (SfM) method on a 0.17 ha region in Wupatki Wash. SfM is a low-cost photogrammetric method that uses digital photographs to create 3-dimensional (3D) surfaces, and has become increasingly popular in geoscience and archaeological applications (e.g., Howland et al., 2018; Westoby et al., 2012; Jones & Church, 2020; Sha et al., 2023). We systematically walked in a grid pattern and used an iPhone 12 attached to a 5-m tall pole (Figure 9). At each grid point, four photographs were taken in orthogonal directions to capture a variety of angles for sufficient overlap to estimate 3D structures from 2D images. Agisoft Metashape Professional (Agisoft, 2020) software was used to create a digital elevation model (DEM) from 2,313 photographs and 24 RTK-surveyed control points. A DEM of difference (DoD) was then created using ArcGIS Pro from topography derived from 2016 aerial LiDAR and 2021 photographs (Wheaton et al., 2010). Within ArcGIS Pro, large vegetation patches were removed from the model to eliminate topographic skew from the DoD analysis. Similar to Sholtes et al. (2018), we created two sample polygon shapefiles on relatively flat and steep areas where we did not expect change to occur to correct for bias and remove values within ± two standard deviations of the error within sampled areas (Wheaton et al., 2010).

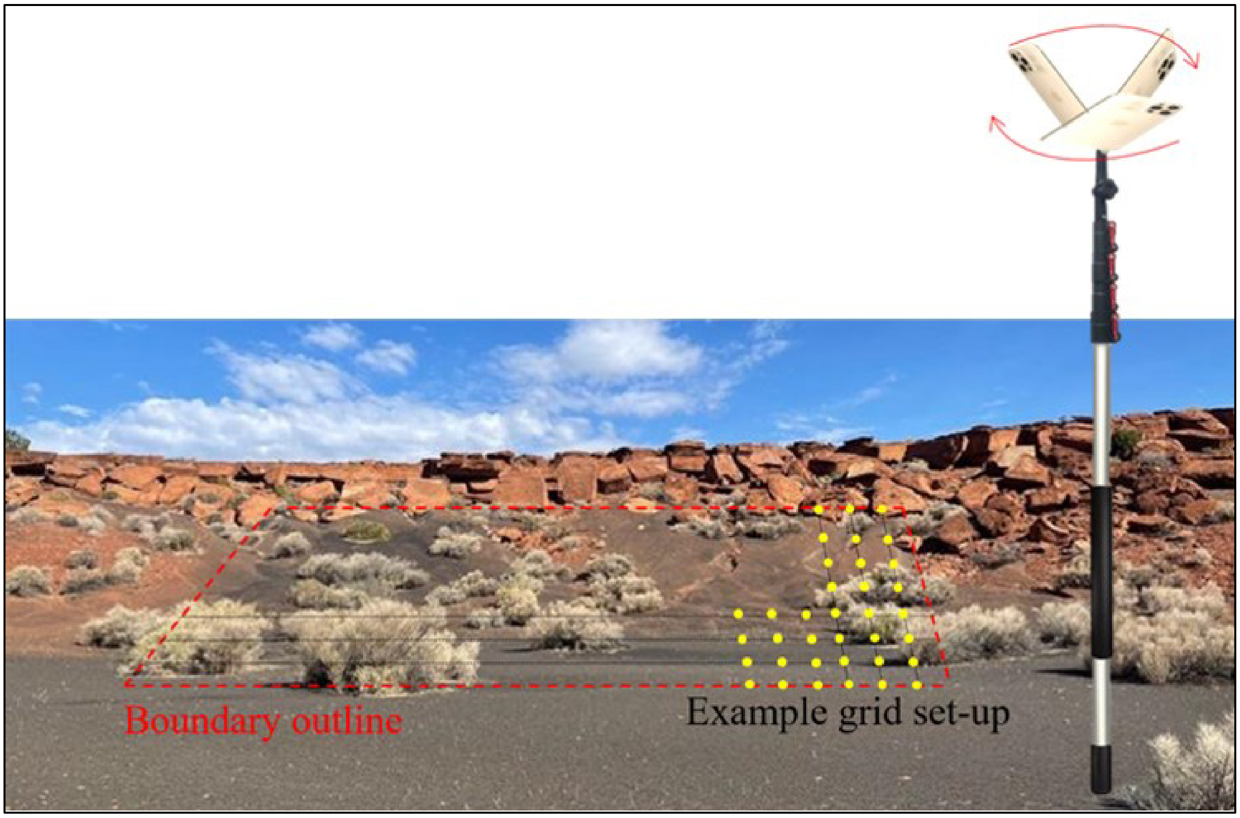

Figure 9. Grid system used for collecting photographs for SfM analysis.

2.3 Archaeological Site Vulnerability Assessment

Archaeological site vulnerability was classified as either high, moderate, low, or unclassified based on proximity to a cliff band or a measured gully (Figure 10**)** for 54 archaeological sites located in the eastern portion of WUPA. Geomorphically, cliff bands are important features in WUPA because as water flows over the vertical face, higher velocities result in erosion of the underlying materials and downslope concentrated flow paths. Gullies readily form within the volcanic cinders that blanket the Moenkopi Formation (Figure 5) below cliff bands. We used the buffer tool in ArcGIS Pro to determine archaeological site proximity to measured gullies and cliff bands. Cliff bands were delineated in ArcGIS Pro using aerial imagery from the National Agriculture Imagery Program (NAIP) that was obtained through the USGS Earth Explorer. If a site was located within 5 m of measured gullies or delineated cliff bands, the archaeological site was given a high erosion vulnerability classification (Figure 10). We chose a conservative buffer of 5 m because of the amount of landscape change observed within the five-year time frame, uncertainty in the coordinates of the archaeological site locations provided, presence of atypical gully head morphology in some locations, and to ensure we captured any archaeological sites with a potential for future erosion. Otherwise, site classification was based on underlying lithology, field observations, or personal communication with NPS staff (Figure 10).

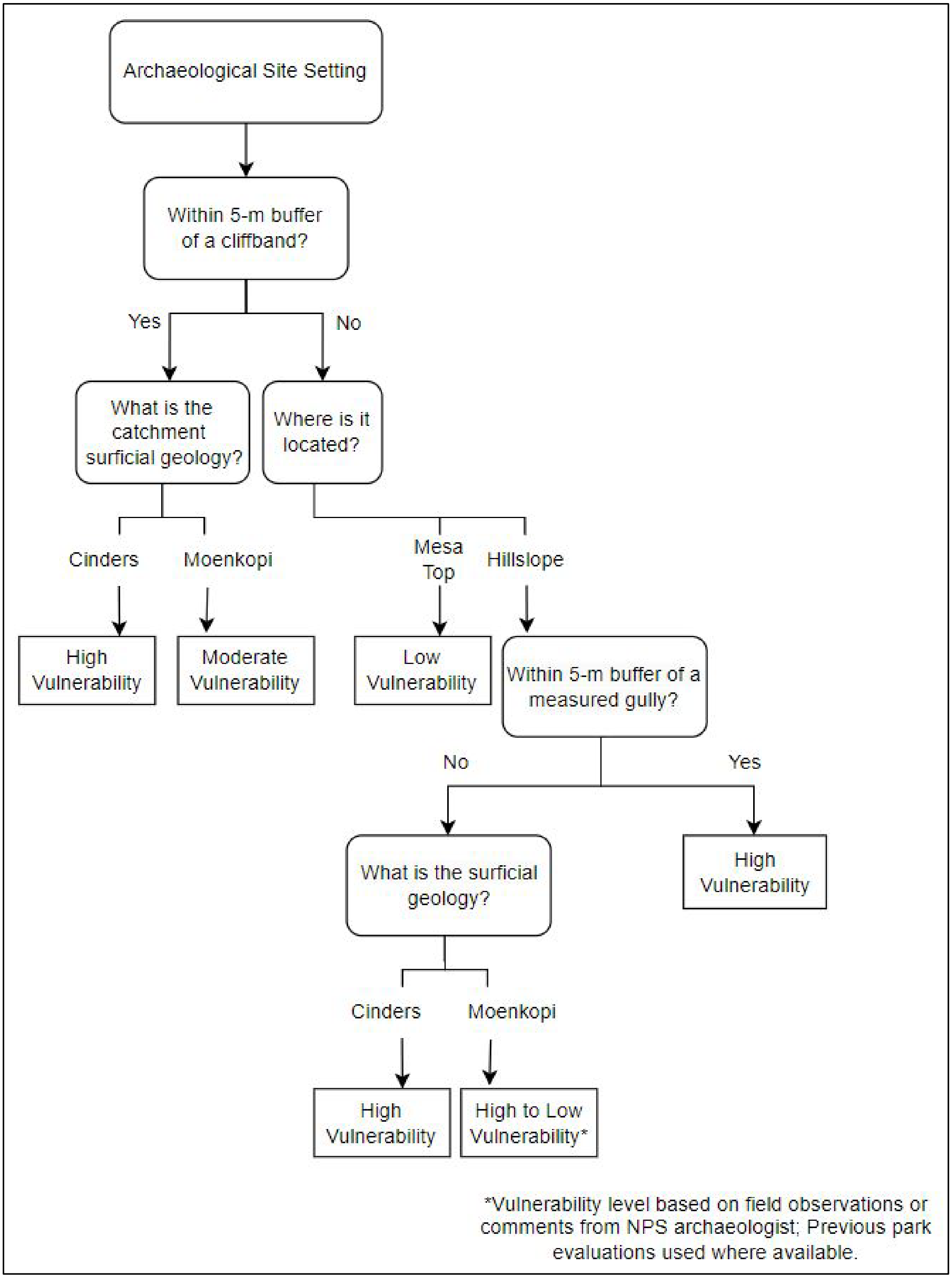

Figure 10. Flowchart used to assign erosion vulnerability classifications to archaeological sites.

Chapter 3. Results

3.1 Cinder and Moenkopi-derived sediment differences

Infiltration data recorded from the infiltrometer are summarized in Figure 11. Water infiltrated quickly into cinder-dominated sediments and resulted in higher cumulative infiltration and faster infiltration rates (slopes of infiltration curves) compared to Moenkopi-dominated sediments (Figure 11). K_{fs} estimates were compared for cinders and Moenkopi-derived sediments of sand, silty clay, and clay (Figure 12). Van Genuchten parameters for sand were used for calculations for cinders based on grain size analyses from sediment samples collected in the field. Cinders showed the highest K_{fs} with an average of 0.21 cm/sec, followed by sand (0.17 cm/sec), silty clay (0.026 cm/sec), and clay (0.012 cm/sec).

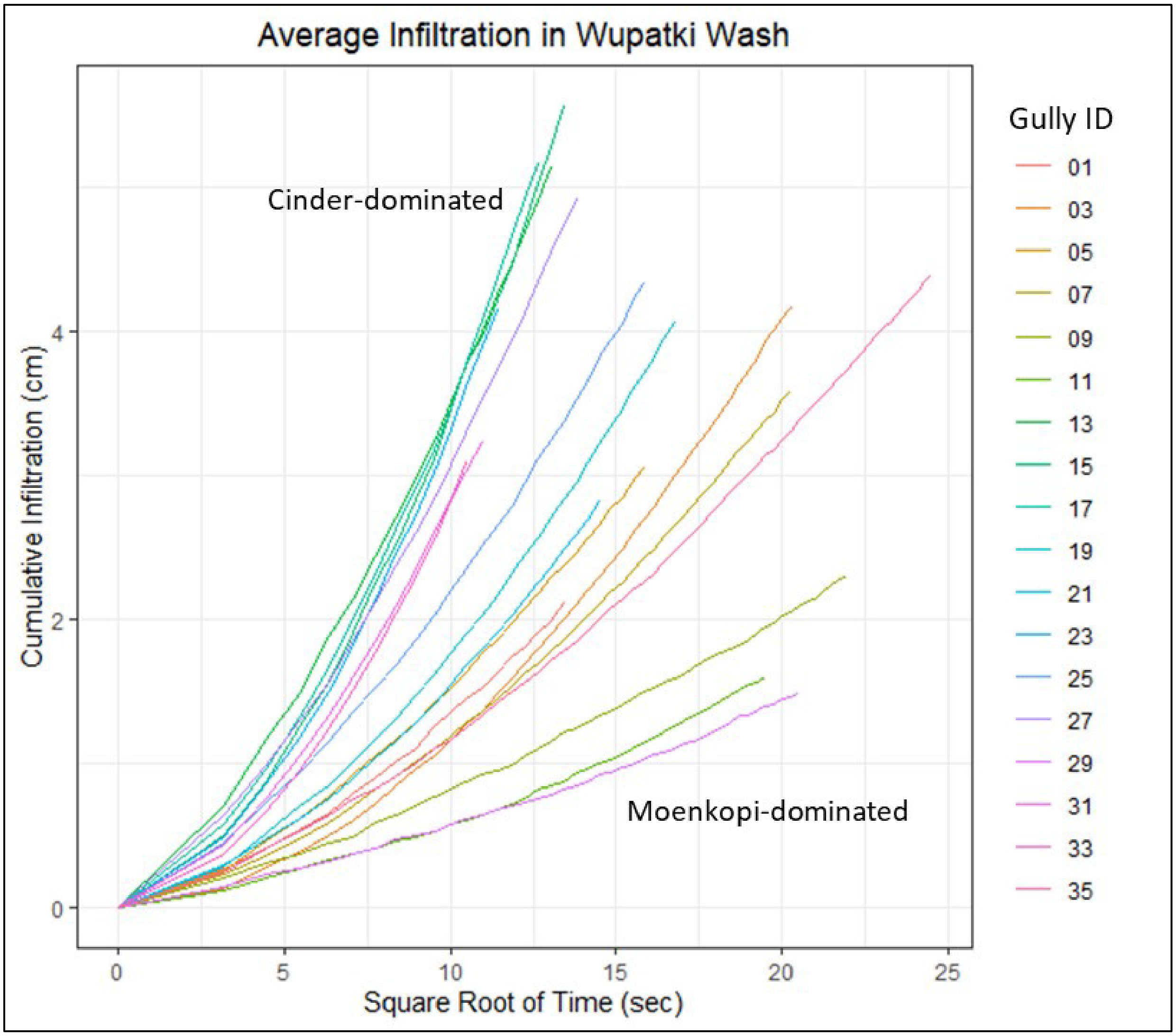

Figure 11. Cumulative infiltration curves from infiltrometer experiments. Less water infiltrated into the Moenkopi-dominated sediments compared to the cinder-dominated, and at a slower rate.

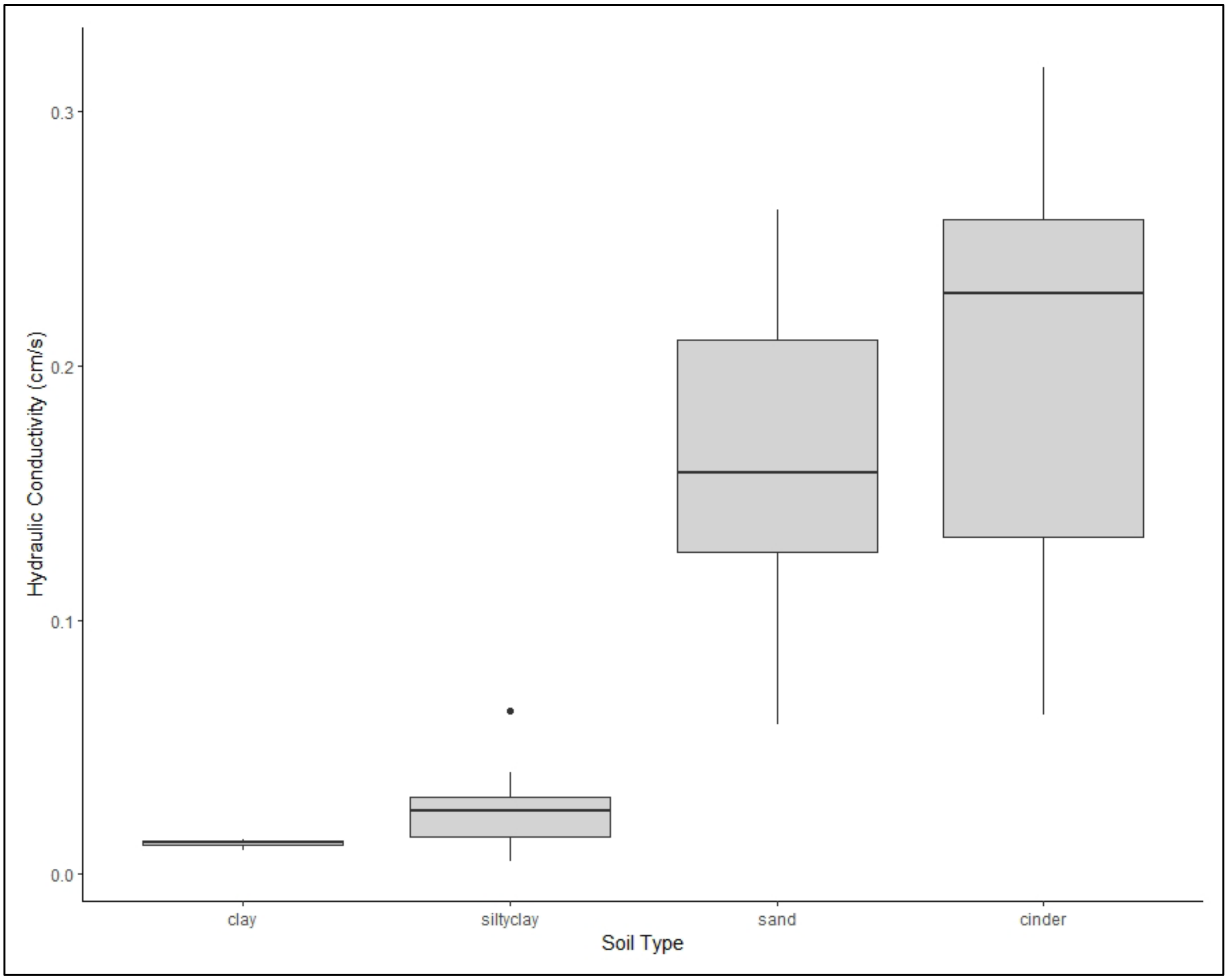

Figure 12. Estimates of hydraulic conductivity for various soil types derived from cumulative infiltration data collected in the field using the infiltrometer. Van Genuchten parameters for sand were used for calculation of hydraulic conductivity of cinders.

A total of 28 sediment samples were sieved from 9 measured gullies. Gullies 8, 26, 28, 31, and 32 were composed of mostly cinders, and gullies 7, 19, 20, and 29 (Figure 7) contained mostly Moenkopi-derived sediments. The average median grain size was 1.01 mm for cinders and 1.48 mm for Moenkopi-derived sediments (Figure 13).

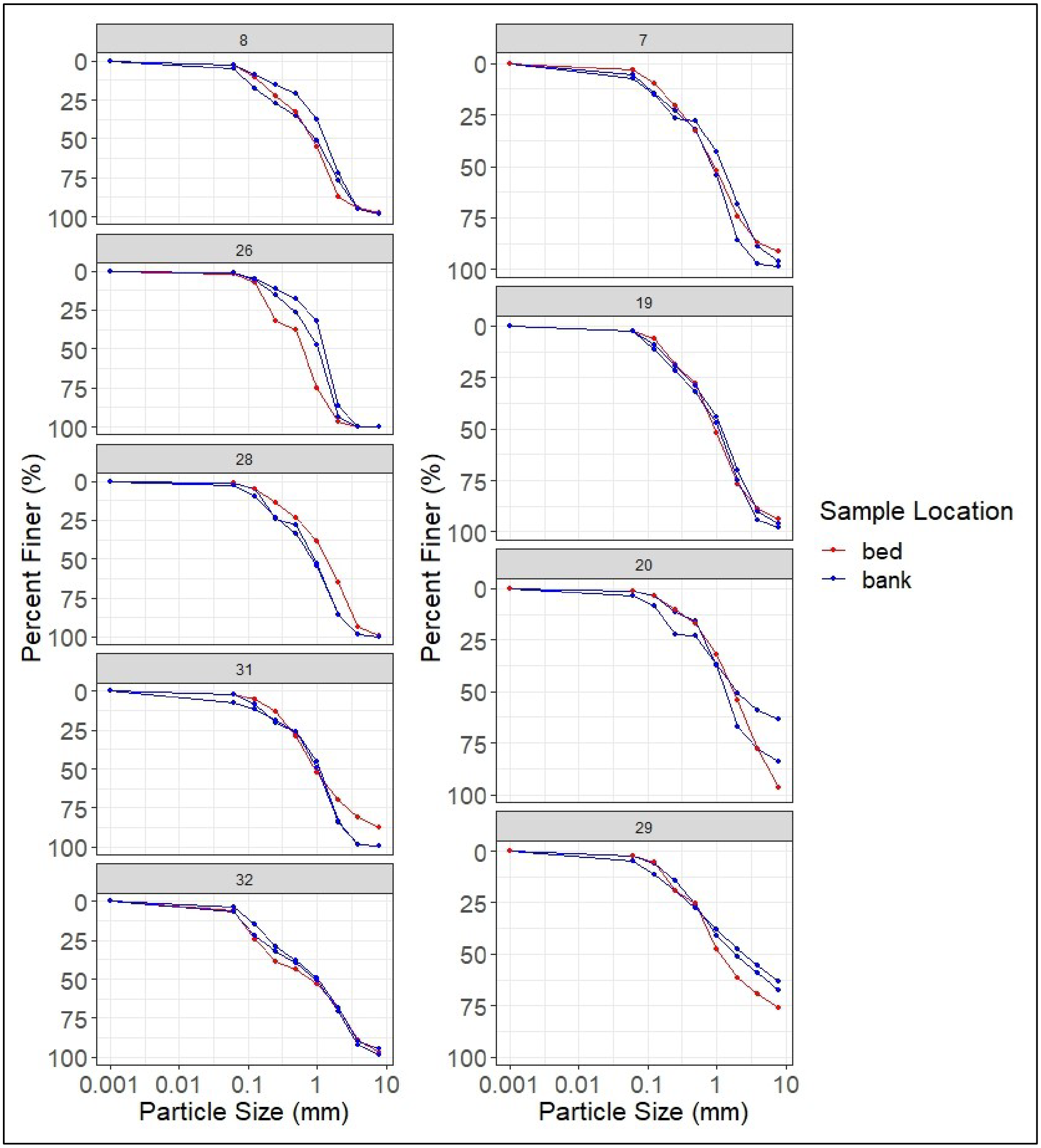

Figure 13. Grain size distribution plots for gullies with bed and banks made of cinders (left) and Moenkopi-sediments (right).

3.2 Catchment Data

Gully catchments included a cliff band of the Moenkopi Formation in 29 of the 35 measured gullies. The cliff band height ranged from 0.1 to 4.9 m, and generally created rockfall blocks in the lower portion of the catchment near gully heads (Figure 5). Catchments generally showed a low percentage of vegetation, but six gullies had a medium percentage of vegetation, and one gully with a high percentage of vegetation. Gully catchment areas ranged from 0.001 to 0.28 ha (Figure 14) and catchment slopes ranged from 0.05 to 0.4 percent. Median catchment area and slope were 0.02 ha and 0.2 percent, respectively. Infiltration data recorded in gully catchments have been reported above in Section 3.1.

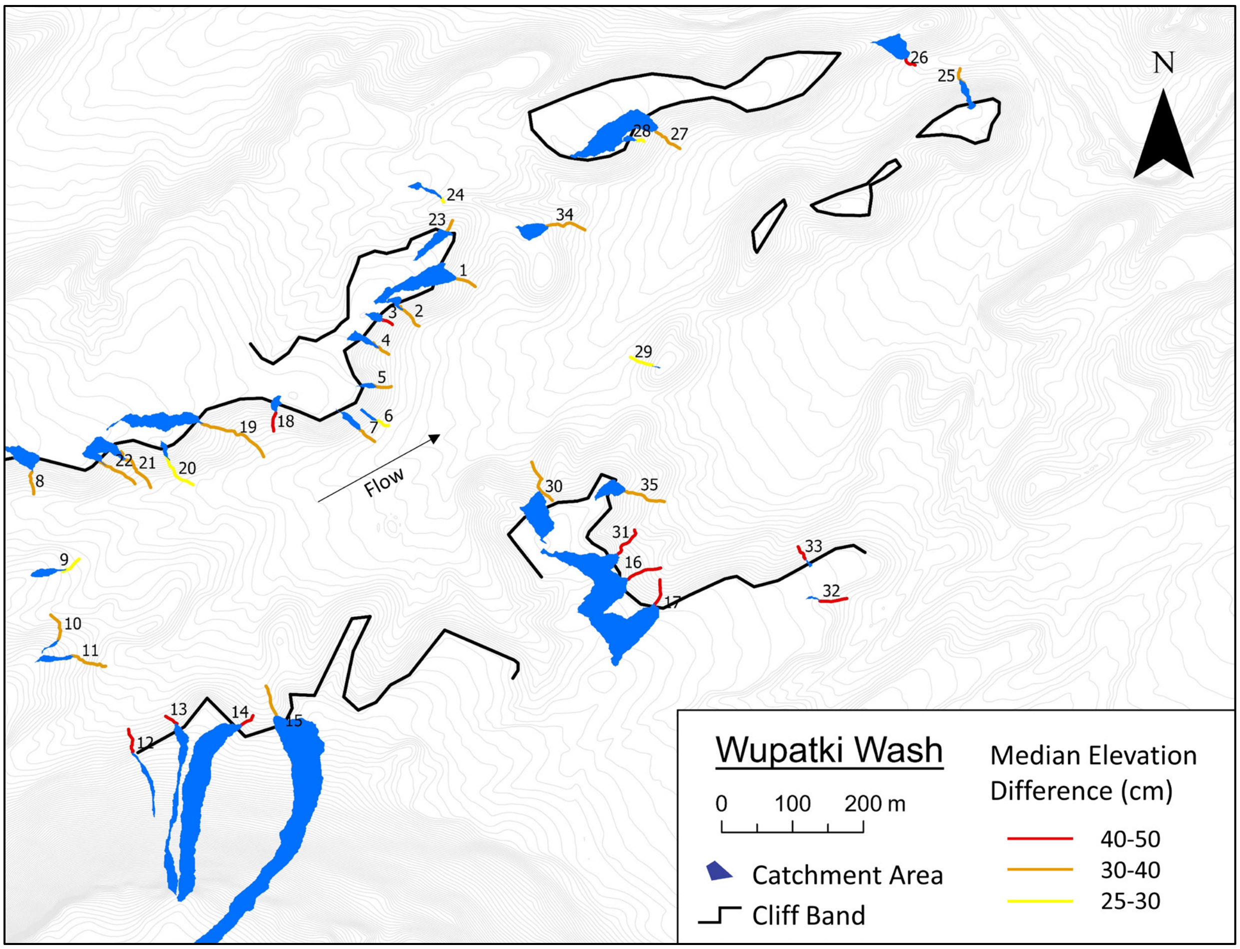

Figure 14. Map of gully catchment areas. The catchment area for gully 15 extends South beyond this image.

3.3 Slope-Area Analysis and Gully Prediction

We plotted our slope and catchment area data against Pederson et al. (2006) because their study was conducted nearby in Grand Canyon National Park (Figure 15). The variables a and b were found to be 0.10 and 0.13, respectively (Figure 15). While the general trend of smaller catchment areas show steeper slopes of Pederson et al. (2006) is visible in our data, our data indicates a much weaker relationship between slope and contributing area (R^2=0.28). As a result, a threshold slope for a given catchment area above which gully erosion occurs in Wupatki Wash has almost negligible utility.

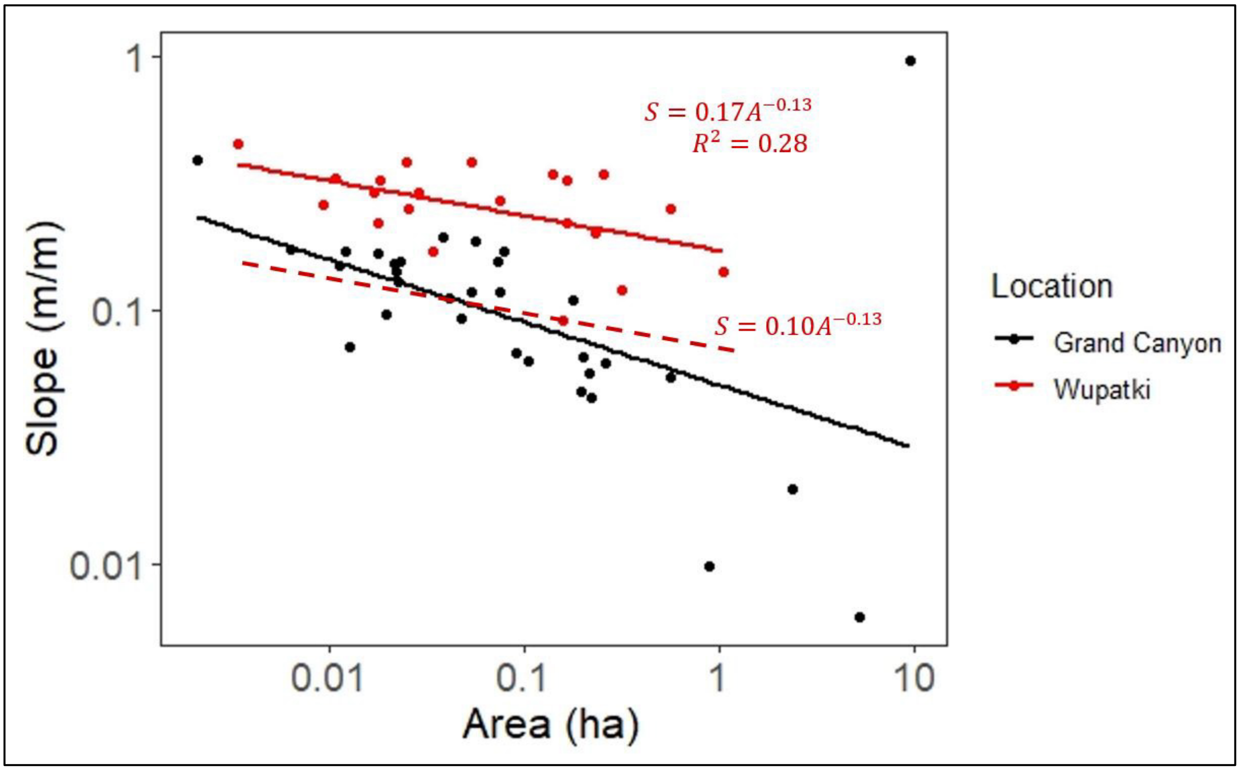

Figure 15. Slope-area relationship for 21 of the 35 measured gullies that all contained cliff bands and formed within cinders. The linear regression (solid red line) was shifted downward to the base of the data to create a gully erosion threshold (dashed red line). The values of the threshold coefficient and scaling exponent are 0.10 and 0.13, respectively. Data collected from Grand Canyon National Park are from Pederson et al. (2006).

3.4 Gully Change Analysis

3.4.1 Width and depth differences from cross-section data

All 35 measured gullies in Wupatki Wash deepened between 2016 to 2021, but only 14 gullies widened (Figure 16). Average width did not change significantly from 2016 to 2021 (p=0.77), but statistically significant changes in average depth occurred (p=<0.001). Six gullies incised on average more than 20 cm, 18 gullies incised more than 10 cm, and the rest showed less than 10 cm of incision (Figure 7, Figure 16). On average, gully 4 narrowed the most by 30 cm, and gully 11 widened the most by 40 cm.

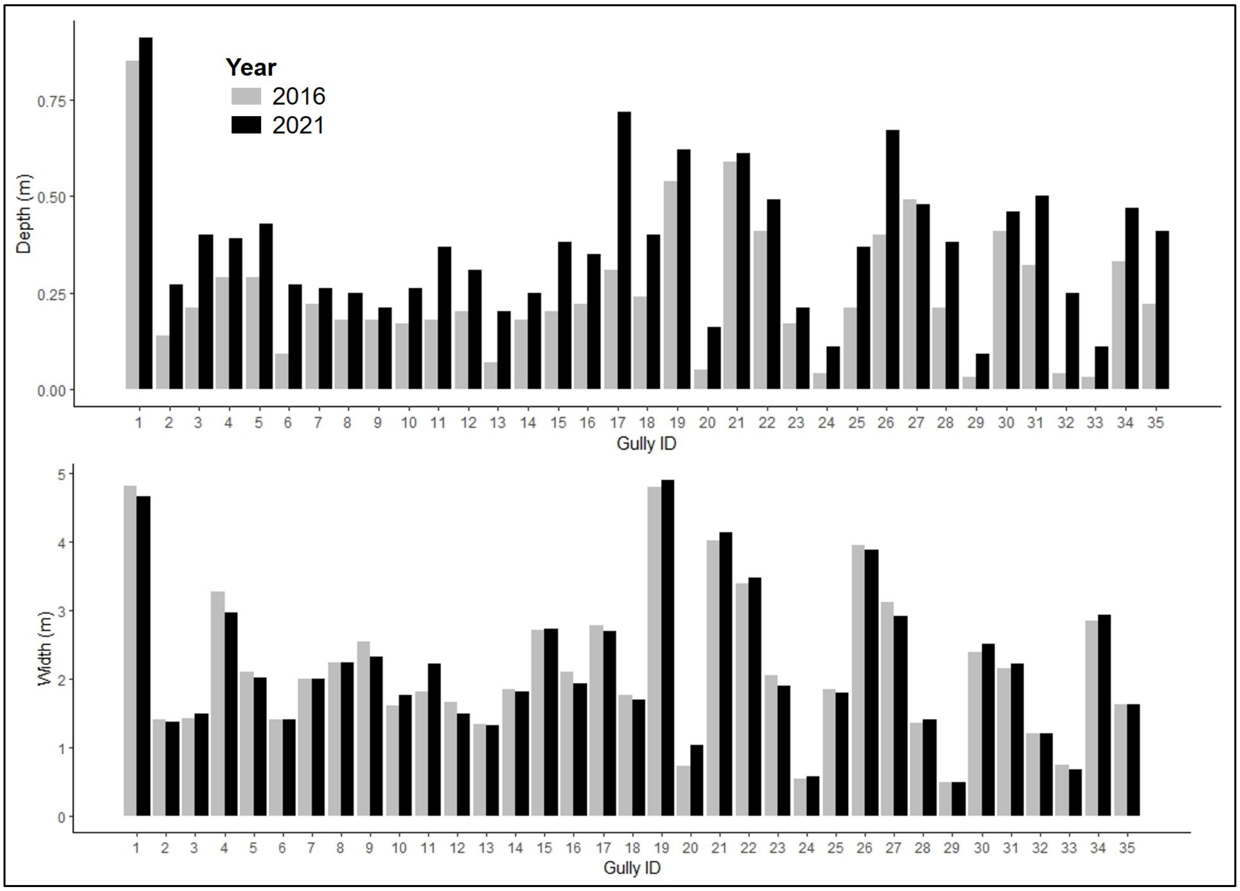

Figure 16. Barplots comparing gully geometries from 2016 to 2021. Gully depth (top) and width (bottom) are shown.

3.4.2 Median Elevation Difference (MED) and slope changes from longitudinal profiles

Consistent with the findings in cross-sectional changes, longitudinal profiles revealed negative MED for all measured gullies (Figure 17). Therefore, all measured gullies have eroded since 2016. Average topographic change was −36 cm and ranged from −52 cm to −25 cm. In addition, the gully slope decreased over the five-year period in 21 of the measured gullies (Figure 18). Gully 23 decreased in slope the most from 0.15 to 0.12, and gully 26 increased in slope the most from 0.14 to 0.15 (Figure 18).

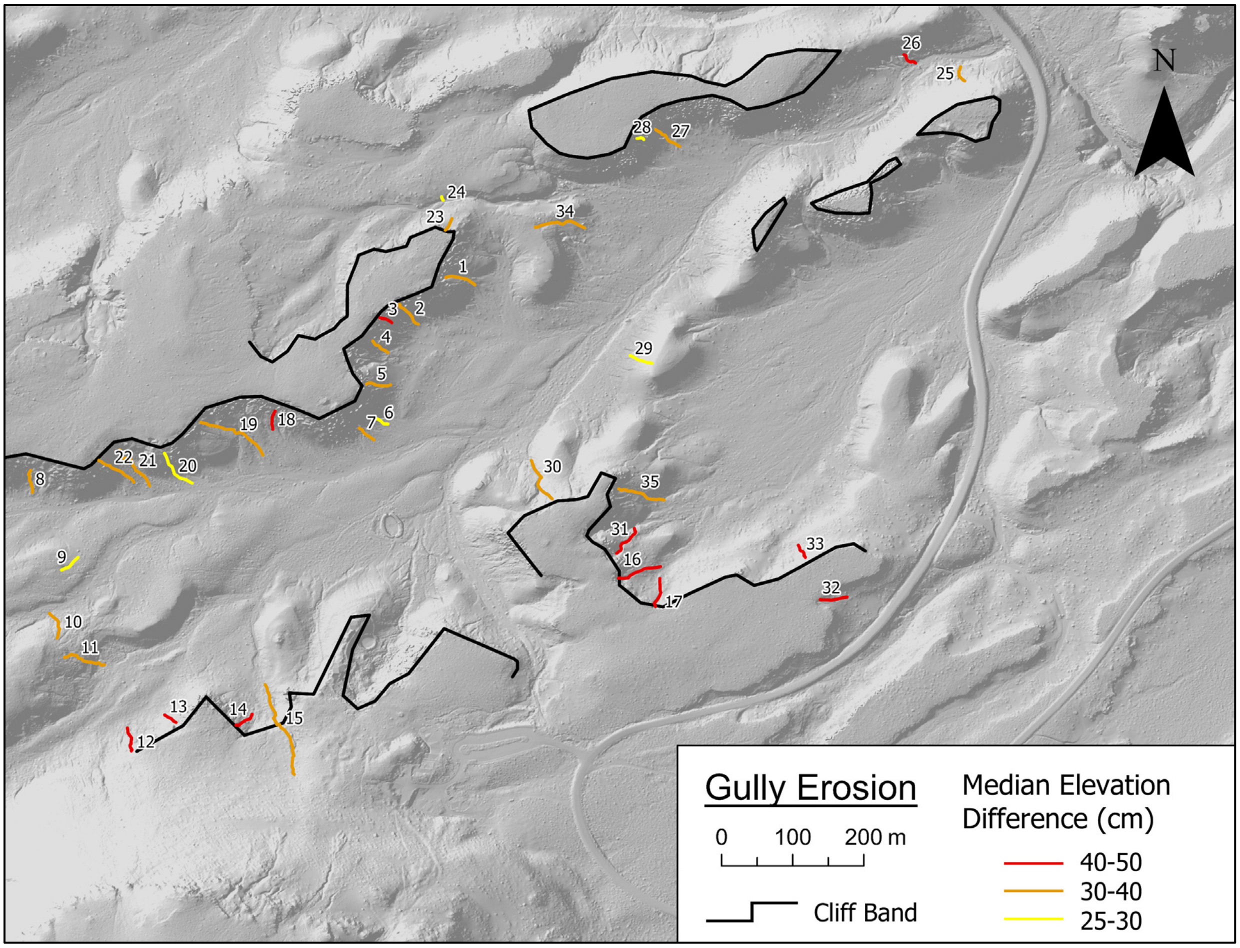

Figure 17. Change in median elevation from 2016 to 2021. All measured gullies had a negative MED suggesting widespread erosion.

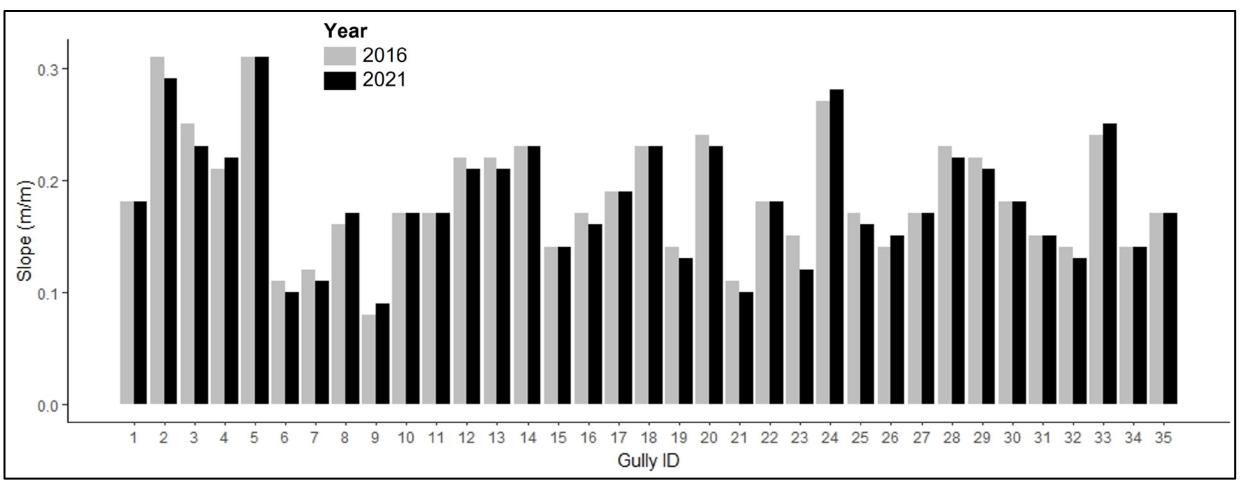

Figure 18. Gully slope changes from 2016 to 2021. The slope of gully 23 changed the most, decreasing from 0.15 to 0.12.

3.4.3 Median Elevation Difference (MED) and slope changes from SfM Analysis

Using SfM and DoD techniques, both incision and depositional processes were observed on the 0.17 ha hillslope in Wupatki Wash over a five-year time frame (Figure 19). Gullies experienced a maximum incision of 0.7 m and maximum deposition of 0.5 m, respectively. Gully incision generally ranged from 0.3 to 0.1 m, but one gully on the northwestern side of the study area filled with cinders with approximately 0.4 m of average deposition (Figure 19). Other depositional zones included the downstream regions of gullies and along gully banks.

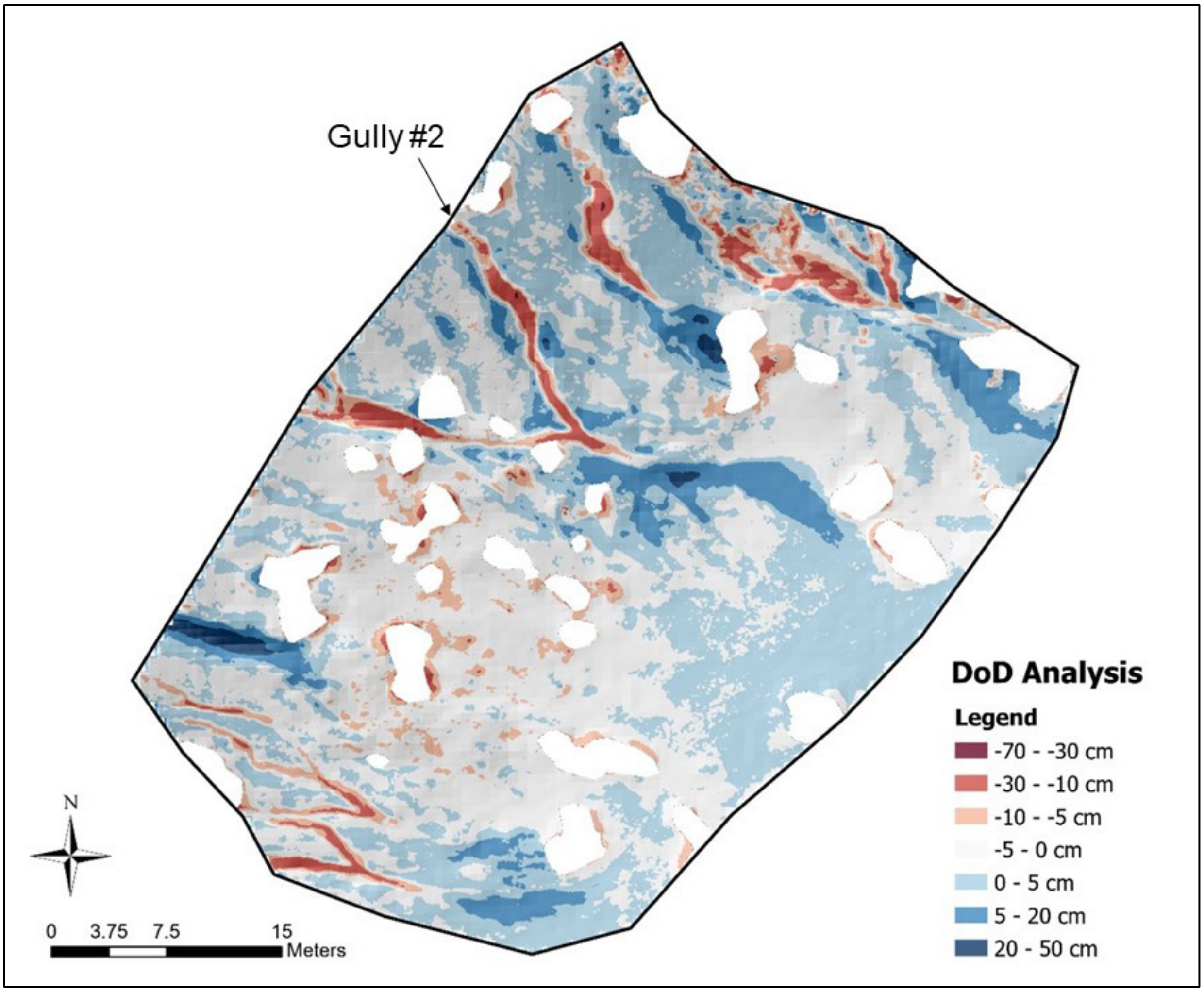

Figure 19. Results from a DEM of Differencing (DoD) analysis using 2016 aerial LiDAR and 2021 iPhone imagery. A semi-transparent hill shade of the 2016 DEM was used as the background. White polygons indicate where vegetation was manually removed from the imagery. Refer to Figure 7 for the location of the DoD analysis.

3.5 Archaeological Site Vulnerability Classification

Archaeological sites were classified for erosion vulnerability using geomorphic and geologic field data (Table 1). Of the 54 sites, 22 were classified in the high category, 14 in the moderate category, and 12 in the low category (Table 1). Seven sites remain unclassified since they were not visited in the field and due to a lack of supporting information. Fifteen sites fell within the cliff band buffer and three sites fell within the measured gully buffer and were given a high vulnerability classification (Figure 10; Table 1). Table 2 summarizes gully rankings and associated archaeological sites that fall within the measured gully buffer.

Table 1. Archaeological site vulnerability assessment based on proximity to cliff bands and measured gullies.

Site Number	Site Type	Location	Vulnerability
WUPA01107	Structure	Within cliff band buffer	High
WUPA01108	Structure	Within gully buffer	High
WUPA01109	Structure	Within cliff band buffer	High
WUPA01110	Structure	Within cliff band buffer	High
WUPA01380	Structure	Unknown; did not visit	Unclassified
WUPA01381	Structure	Within gully buffer	High
WUPA01383	Habitation, Protected	Below cliff band	High
WUPA01384	Habitation, Protected	Within cliff band buffer	High
WUPA01387	Habitation, Protected	Within cliff band buffer	High
WUPA01388	Structure, Other	Moenkopi hillslope	Moderate
WUPA01395	Habitation, Open Air	Mesa top	Low
WUPA01400	Habitation, Open Air	Moenkopi hillslope	Moderate
WUPA01404	Structure	Moenkopi hillslope	Low
WUPA01406	Structure	Moenkopi hillslope	Moderate
WUPA01407	Structure	Moenkopi hillslope	Moderate
WUPA01410	Other	At downstream end of gully 30	Moderate
WUPA01412	Other	Unknown; did not visit	Unclassified
WUPA01413	Structure	Cinder hillslope	High
WUPA01414	Structure	Within cliff band buffer	High
WUPA01418	Structure	Moenkopi hillslope	Moderate
WUPA01419	Structure, Other	Mesa top	Low
WUPA01430	Habitation, Open Air	On very small hillslope	Low
WUPA01431	Structure	Cinder hillslope	High
WUPA01433	Structure	Moenkopi hillslope	Moderate
WUPA01434	Habitation	Moenkopi hillslope	Moderate
WUPA01439	Structure, Other	Moenkopi hillslope	Low
WUPA01442	Structure	Mesa top	Low

* Classification based on NPS archaeologist comments.

Table 1 (continued). Archaeological site vulnerability assessment based on proximity to cliff bands and measured gullies.

Site Number	Site Type	Location	Vulnerability
WUPA01444	Structure	Moenkopi hillslope	Moderate
WUPA01445	Habitation	Within cliff band buffer	High
WUPA01446	Structure	Within cliff band buffer	High
WUPA01447	Habitation	Within gully buffer	High
WUPA01448	Habitation	Moenkopi hillslope	Moderate
WUPA01448	Habitation	Moenkopi hillslope	Moderate
WUPA01449	Structure	Moenkopi hillslope	Moderate
WUPA01454	Structure	Moenkopi hillslope	Moderate
WUPA01455	Structure, Other	On cinder hillslope beneath rock fall	High*
WUPA01457	Habitation, Protected	Within cliff band buffer	High
WUPA01458	Structure	Within cliff band buffer	High
WUPA01459	Structure, Other	On Moenkopi hillslope beneath rock fall	Moderate*
WUPA01494	Structure	Mesa top	Low
WUPA01495	Burial/Grave/Inhumation	Unknown; did not visit	Unclassified
WUPA01496	Artifact Scatter	Unknown; did not visit	Unclassified
WUPA01497	Structure, Other	Within cliff band buffer	High
WUPA01498	Structure, Other	Unknown; did not visit	Unclassified
WUPA01499	Structure, Other	Thin layer of cinders overlaying Moenkopi bedrock	Low*
WUPA01500	Habitation, Protected	Mesa top	Low
WUPA01511	Structure, Other	Within cliff band buffer	High
WUPA01512	Habitation, Protected	Shallow cinder basin	Low*
WUPA01513	Structure, Other	Within cliff band buffer	High
WUPA01518	Structure	Unknown; did not visit	Unclassified
WUPA01519	Habitation	Within cliff band buffer	High
WUPA01520	Structure, Other	Within cliff band buffer	High
WUPA01521	Habitation, Open Air	Unknown; did not visit	Unclassified
WUPA01522	Check Dam	Adjacent to WUPA wash tributary bed	Low*
WUPA02674	Habitation, Open Air	Mesa top	Low

* Classification based on NPS archaeologist comments.

Table 2. A summary table of gully catchment characteristics and erosion ranking of yellow, orange, and red based on the change in median elevation (Figure 17). Additionally, archaeological sites that fell within the buffered region of a gully are provided.

Gully ID	Average Cliff Height (m)	Vegetation Cover in Catchment [A]	Catchment Material	Median Elevation Difference (m)	Archaeological Sites Within Buffer
1	1.6	low	Moenkopi	−0.351 [C]	–
2	2.0	low	Thin cinder cover	−0.337 [C]	–
3	1.9	low	Moenkopi	−0.431 [B]	–
4	2.2	low	Moenkopi	−0.344 [C]	–
5	2.3	low	Moenkopi	−0.343 [C]	–
6	2.0	medium	Moenkopi	−0.309 [D]	–
7	1.8	low	Moenkopi	−0.337 [C]	–
8	3.1	low	Thin cinder cover	−0.360 [C]	–
9	0	low	Moenkopi	−0.288 [D]	–
10	0	low	Blue-grey basaltic fragments with cinders	−0.325 [C]	–
11	0.9	medium	Blue-grey basaltic fragments with cinders	−0.327 [C]	–
12	1.8	medium	Thin cinder cover	−0.432 [B]	–
13	2.3	low	Cinders	−0.423 [B]	WUPA01381
14	0.9	low	Cinders	−0.493 [B]	–
15	2.5	high	Cinders	−0.381 [C]	–
16	2.0	low	Thin cinder cover	−0.440 [B]	–
17	1.8	medium	Cinders	−0.509 [B]	–
18	1.7	low	Thin cinder cover	−0.418 [B]	WUPA01447
19	2.8	medium	Thin cinder cover	−0.311 [C]	–
20	0.7	low	Thin cinder cover	−0.274 [D]	–
21	1.9	medium	Cinders	−0.327 [C]	WUPA01108
22	2.8	low	Moenkopi	−0.318 [C]	–
23	1.1	low	Cinders	−0.352 [C]	–
24	0.1	low	Moenkopi	−0.278 [D]	–
25	4.9	low	Moenkopi	−0.356 [C]	–
26	0	low	Moenkopi	−0.468 [B]	–
27	1.1	low	Cinders	−0.336 [C]	–
28	1.2	low	Thin cinder cover	−0.302 [D]	–

[A] Vegetation cover was recorded as a percentage from 0–100% and then classified as low (0–30%), medium (31–70%), and high (71–100%).

[B] Gullies ranked red eroded on average from 40–50 cm.

[C] Gullies ranked orange eroded on average from 30–40 cm.

[D] Gullies ranked yellow eroded on average from 25–30 cm.

Table 2 (continued). A summary table of gully catchment characteristics and erosion ranking of yellow, orange, and red based on the change in median elevation (Figure 17). Additionally, archaeological sites that fell within the buffered region of a gully are provided.

Gully ID	Average Cliff Height (m)	Vegetation Cover in Catchment [A]	Catchment Material	Median Elevation Difference (m)	Archaeological Sites Within Buffer
29	0	low	Moenkopi	−0.283 [D]	–
30	1.5	low	Moenkopi	−0.355 [C]	–
31	1.4	low	Thin cinder cover	−0.539 [B]	–
32	0.4	low	Cinders	−0.453 [B]	–
33	1.0	low	Cinders	−0.435 [B]	–
34	0.0	low	Moenkopi	−0.325 [C]	–
35	1.2	low	Moenkopi	−0.376 [C]	–

[A] Vegetation cover was recorded as a percentage from 0–100% and then classified as low (0–30%), medium (31–70%), and high (71–100%).

[B] Gullies ranked red eroded on average from 40–50 cm.

[C] Gullies ranked orange eroded on average from 30–40 cm.

[D] Gullies ranked yellow eroded on average from 25–30 cm.

Chapter 4. Discussion and Conclusions

4.1 Discussion

4.1.1 Erosion Threshold

The threshold model of erosion suggests that gully formation is controlled by the balance between erosion and deposition of sediment in a watershed, which is influenced by the characteristics of the contributing area. Larger contributing areas have a greater capacity to store water and generate runoff, which reduces the slope angle required to initiate gully erosion. As a result, gullies in larger contributing areas tend to have shallower slopes (Figure 15). Conversely, smaller contributing areas have less capacity to store water and generate runoff, which increases the slope angle required to initiate gully erosion. As a result, gullies in smaller contributing areas tend to have steeper slopes. In Wupatki Wash, however, the slope-area relationship is weak and gullies with smaller catchments degrade at a comparable rate as gullies with larger catchments. Thus, our hypothesis about the slope-area relationship was not supported by the data, and we did not find a threshold slope above which gully erosion occurs. We attribute the lack of a strong slope-area relationship found in other studies (e.g., Patton and Schumm, 1975; Montgomery and Dietrich, 1994; Pederson et al., 2006; Wu and Cheng, 2005) to lithological differences and, in particular, the high mobility and permeability of cinders. While the negative slope-area trend normally implies overland flow-driven processes, the weak trend seen at WUPA suggests subsurface flow (through the cinders) is influencing erosion (Vanderkerchove et al., 2000). The slope-area topographic relationship is not sufficient for explaining an erosion threshold at WUPA. Our data are comparable to the spread of contributing areas of Pederson et al. (2006), but the range of slopes of our data is much less (Figure 15).

4.1.2 Gully Morphology and Change Analysis

In Wupatki Wash, there is no evidence of head cut retreat in gullies. Gully heads are either abrupt at a cliff band or gradual after rockfall debris (Figure 5 and 6). In either case, gully heads remain fixed in position, while changes in gully slope (Figure 18) result from either erosion or aggradation. Gully heads remain fixed in position such that they cannot retreat because of the presence of the rockfall and cliff band in the catchment. Where gully heads are abrupt, the dominant process of gully erosion is pour-over that occurs from runoff over the cliff band (Figure 5 and 6). Slope breaks (gully knickpoints) did occur within gullies where Moenkopi sandstone outcropped, or Moenkopi colluvium accumulated within the gully bed. We found gullies to form primarily within cinder deposits with steeply sloped sides but not steep head cuts (Figure 6). Cross-sectional shape is a function of soil material type, and gully evolution (Thwaites et al., 2021). The gullies at WUPA are 'V' shaped (Figure 6), suggesting gullies form in materials with a high level of aggregate stability (Downes, 1946), and the gully is in the channel-eroding or stabilized stage of development (Ireland et al., 1939). However, models of gully development are typically based on weaker materials overlain by a more resistant material (Ireland et al., 1939; Schumm, 1960), which does not apply to WUPA. Generally, we observed gullies form within less-resistant cinders overlying more resistant silty sandstone (Figure 8). Cinders do not have a high level of aggregate stability, but gully banks did appear relatively stable at the cinder's angle of repose. The angle of repose of cinders is comparable to that of sand, around 30° (Porter, 1972). Bank collapse was evident in some gullies between patches of vegetation or where Moenkopi bedrock affected the bank. We did not examine gully vegetation cover within the analysis because only one measured gully had a high amount of vegetation in the catchment and vegetation presence on gully banks was generally very minimal.

As opposed to channel widening from bank undercutting and failure (Pederson et al., 2006), gullies in Wupatki Wash have eroded primarily by channel incision (Figure 16 and 19). Some gullies contained pieces of Moenkopi colluvium or bedrock within the channel bed, however, which would limit further incision. All measured gullies were eroding, but as seen in Figure 19, some gullies at WUPA may be aggrading. Almost all measured gullies contained cliff bands, and we attribute gully erosion to runoff effects following rain events. Where cinders are present in catchments, runoff-generation is likely from saturation-excess overland flow due to the cinder's high permeability. Additionally, cinders are likely transported as a slurry and runoff over cliff bands into downstream gullies. Intermittent debris flows may occur given a sufficiently high rainfall intensity. The lower infiltration rate of Moenkopi-derived sediments suggests infiltration-excess overland flow likely leads to quicker runoff focused into gullies. Cinders are very loose, friable, non-cohesive, and mobile compared to Moenkopi-sediments. They are also slightly finer in grain size (Figure 13). Therefore, cinders are detached and transported more easily. For this reason, catchments composed of primarily cinders were found to have larger MEDs than those with surficial Moenkopi-sediments (Figure 17). This was an unexpected result, however, as we hypothesized Moenkopi-dominated catchments would increase the magnitude of runoff and MED. Thus, our second hypothesis was also not supported. Depth of cinders was not measured in the field, but we believe is an important control on erosion. Gullies with higher MEDs formed within thick cinder deposits. In addition to water erosion, cinders erode from aeolian processes, but these processes were not evaluated in this investigation.

4.1.3 Vulnerability Assessment

A 5-m buffered region around cliff band and measured gullies was used to designate archaeological sites as highly vulnerable to erosion, regardless of surficial catchment lithological properties. These sites experience direct impact from runoff over cliff bands and erosion was observed in all measured gullies. Three other sites (WUPA01455, WUPA01431, and WUPA01413) were given high vulnerability classifications because they are found on cinder hillslopes, which erode more readily compared to hillslopes composed of Moenkopi-sediments (Table 1). Moderate and low classifications varied based on site setting, surficial geology, field notes, or field observations from an NPS archaeologist. These classifications were primarily based on lithology and site setting, but additional factors including flow accumulation, local slope, and presence of vegetation could be used to improve archaeological site classifications. Although a large amount of baseline geomorphic data was collected, the classification of archaeological sites was constrained by limited accessibility to measure specific gullies. This analysis could be improved by collecting aerial imagery and performing a large-scale, high spatial resolution landscape change detection analysis to further evaluate archaeological site vulnerability.

4.2 Conclusions

This study analyzed gully morphologic changes over a five-year period and classified archaeological sites based on vulnerability to gully erosion. Baseline geomorphological data collected in the summer of 2021 revealed an eroding landscape at WUPA. According to the coarse-scale analysis using longitudinal profile data, all measured gullies showed a negative MED, with a maximum of 50 cm of incision. These data were corroborated with cross-section data, where average gully depth was significantly greater in 2021 than 2016 for all measured gullies ($p<0.001$). Although statistically significant changes in width were not found, these results provided insight into gully development and growth.

We linked catchment surficial geology to gully erosion, with unexpected results. Although water infiltrated quickly through the cinders, more erosion occurred in gullies with catchments predominantly covered with cinders. Additionally, cinders likely influence gully slope because the size of the catchment was weakly related to the gully head slope. In a semi-arid environment like WUPA, surficial geology, particularly the presence of Moenkopi Formation cliffs, heavily influences runoff processes and gully erosion. With changing precipitation patterns due to a warming climate, we recommend park managers focus monitoring efforts based on the geomorphic-controlled gully and archaeological site classifications. A total of 22 sites were classified as high vulnerability based on our analysis and flow diagram.

Chapter 5. Literature Cited

AgiSoft PhotoScan Professional (Version 1.6.1) (Software). 2020. Retrieved from https://www.agisoft.com/downloads/installer/.

Anderson, K. 2021. Wupatki Pueblo Geoarcheology Landscape Assessment.

ASTM International. 2018. Standard test methods for particle-size distribution (gradation) of soils using sieve analysis (ASTM D6913-17). ASTM International.

Aquaveo. 2022. WMS: Watershed modeling system [Computer software]. https://www.aquaveo.com/software/wms-watershed-modeling-system.

Baldwin, L., Cultural, M. A., and Program Manager, R. 2015. Archeological Excavation at WS1109, Structure 2 Wupatki National Monument Sunset Crater, Walnut Canyon and Wupatki National Monuments Cultural Resource Division FOIA Exempt: For Internal Use Only Archeological Excavation at WS1109 Structure 2 Wupatki National Monument.

Billingsley, G. H., S. S. Priest, and T. J. Felger. 2007. Geologic map of Wupatki National Monument and vicinity, Coconino County, Northern Arizona.

Decagon Devices. 2014. Mini Disk Infiltrometer Model S Manual.

Dóniz, J., C. Romero, J. Carmona, and A. García. 2011. Erosion of cinder cones in Tenerife by gully formation, Canary Islands, Spain. Physical Geography 32(2): 139–160. https://doi.org/10.2747/0272-3646.32.2.139

Downes, R. G. 1946. Tunnelling erosion in north-eastern Victoria. Journal of the Council for Scientific and Industrial Research 19: 283–292.

Emmett, W. W. 1968. Gully erosion, Fairbridge, R.W., ed., Encyclopedia of geomorphology. New York, Reinhold, p. 517–519.

Grattan, J., and R. Torrence. 2007. Living under the shadow: Cultural impacts of volcanic eruptions. Left Coast Press.

Gouma, M., G. J. van Wijngaarden, and S. Soetens. 2011. Assessing the effects of geomorphological processes on archaeological densities: A GIS case study on Zakynthos Island, Greece. Journal of Archaeological Science 38(10): 2714–2725. https://doi.org/10.1016/j.jas.2011.06.009

Hansen, M., J. Coles, K. A. Thomas, D. Cogan, M. Reid, J. Von Loh, and K. Schulz. 2004. USGS-NPS National Vegetation Mapping Program: Wupatki National Monument, Arizona, Vegetation Classification and Distribution Final Report.

Hanson, S. L. 2003. Roadside geology: Wupatki and Sunset Crater Volcano National Monuments. Arizona Geological Survey.

Higgins, C. G., B. R. Hill, and A. K. Lehre. 1990. Gully development. Special Paper of the Geological Society of America 252: 139–155. https://doi.org/10.1130/SPE252-p139

Howland, M. D., I. W. N. Jones, M. Najjar, and T. E. Levy. 2018. Quantifying the effects of erosion on archaeological sites with low-altitude aerial photography, structure from motion, and GIS: A case study from southern Jordan. Journal of Archaeological Science 90: 62–70. https://doi.org/10.1016/j.jas.2017.12.008

Hooten, J. A., M. H. Ort, and M. D. Elson. 2001. Origin of cinders in Wupatki National Monument. Technical Report No. 2001-12. Desert Archaeology, Inc., Tucson, Arizona.

Ireland, H. A. (Hubert Andrew), Sharpe, C. F. Stewart (Charles Farquharson Stewart), and D. H. Eargle. 1939. Principles of gully erosion in the Piedmont of South Carolina. Washington: U.S. Dept. of Agriculture.

Jones, C. A., and E. Church. 2020. Photogrammetry is for everyone: Structure-from-motion software user experiences in archaeology. Journal of Archaeological Science: Reports, 30. https://doi.org/10.1016/j.jasrep.2020.102261

Langbein, W. B., and S. A. Schumm. 1958. Yield of sediment in relation to mean annual precipitation. Transactions, American Geophysical Union 39: 1076–1084.

Montgomery, D. R., and W. E. Dietrich. 1994. Landscape dissection and contributing area-slope thresholds — Chapter 11. *In*: Kirkby, M. J. (Ed.). Process models and theoretical geomorphology. John Wiley & Sons Ltd, pp. 221–246.

NOAA. (n.d.). Percent Frequency Distribution Spreadsheet - 02-9542 (Flagstaff, AZ). National Weather Service. https://hdsc.nws.noaa.gov/hdsc/pfds/pfds_printpage.html?st=az&sta=02-9542&data=depth&units=english&series=pds#table

Patton, P. C., and S. A. Schümm. 1975. Gully erosion, northwestern Colorado: A threshold phenomenon. http://pubs.geoscienceworld.org/gsa/geology/article-pdf/3/2/88/3521842/i0091-7613-3-2-88.pdf

Pederson, J. L., P. A. Petersen, and J. L. Dierker. 2006. Gullying and erosion control at archaeological sites in Grand Canyon, Arizona. Earth Surface Processes and Landforms 31(4): 507–525. https://doi.org/10.1002/esp.1286

Petersen, P. A. 2003. Mitigation, monitoring, and geomorphology related to gully erosion of archaeological sites in Grand Canyon. MS Thesis, Utah State University, Logan, Utah.

Porter, S. 1972. Distribution, morphology, and size frequency of cinder cones on Mauna Kea Volcano, Hawaii. Geological Society of America Bulletin 83(12): 3607–3612. https://doi.org/10.1130/0016-7606(1972)83[3607:DMASFO]2.0.CO;2

Sha, G., G. Shu, Y. Xiping, et al. Mobile phone imaging point cloud modelling for 3D recording and measurement of small scenes of suspected fossil outcrops found in the field. Geoheritage 15: 33 (2023). https://doi.org/10.1007/s12371-022-00780-y

Sholtes, J. S., S. E. Yochum, J. A. Scott, and B. P. Bledsoe. 2018. Longitudinal variability of geomorphic response to floods. Earth Surface Processes and Landforms 43(15): 3099–3113. https://doi.org/10.1002/esp.4472

Schumm, S. A., M. D. Harvey, and C. C. Watson. 1984. Incised channels: Morphology, dynamics, and control. Littleton, Colo: Water Resources Publications.

Tarboton, D. 1997. A new method for the determination of flow directions and contributing areas in grid digital elevation models. Water Resources Research 33: 309–319.

Thwaites, R. N., A. P. Brooks, T. J. Pietsch, and J. R. Spencer. 2021. What type of gully is that? The need for a classification of gullies. Earth Surface Processes and Landforms (October 2020), 1–20. https://doi.org/10.1002/esp.5291

Vandekerckhove, L., J. Poesen, D. O. Wijdenes, J. Nachtergaele, C. Kosmas, M. J. Roxo, and T. De Figueiredo. 2000. Thresholds for gully initiation and sedimentation in Mediterranean Europe. Earth Surface Processes and Landforms 25(11): 1201–1220.

Westoby, M. J., J. Brasington, N. F. Glasser, M. J. Hambrey, and J. M. Reynolds. 2012. “Structure-from-Motion” photogrammetry: A low-cost, effective tool for geoscience applications. Geomorphology 179: 300–314. https://doi.org/10.1016/j.geomorph.2012.08.021

Wheaton, J. M., J. Brasington, S. E. Darby, and D. A. Sear. 2010. Accounting for uncertainty in DEMs from repeat topographic surveys: Improved sediment budgets. Earth Surface Processes and Landforms 35(2): 136–156. https://doi.org/10.1002/esp.1886

Wu, Y., and H. Cheng. 2005. Monitoring of gully erosion on the Loess Plateau of China using a global positioning system. Catena 63 154–166.

Appendix A

From the slope-Area analysis, we created a threshold model and predicted where gullies form on hillslopes (Figure A1). The model performed well and predicted locations of measured gullies. Similar to Pederson et al. (2006), the threshold model overpredicts gully channelization and lacks site-specific influences (e.g., infiltration rate of various lithologies). In a few cases, the banks of large, steep-sided gullies were predicted instead of the channel bed. Several rills through Moenkopi-sediments (no cinders present within the gully) were measured but were not included in the slope-area analysis. As such, the model did not predict the locations of these measured incisional features. The presence of large rockfall debris beneath cliff bands resulted in steep "actual" slopes and thus could potentially be removed to improve the prediction map. We collected baseline geomorphic data for this analysis, but with additional data collection, such a threshold model could prove useful for predicting areas vulnerable to gully erosion.

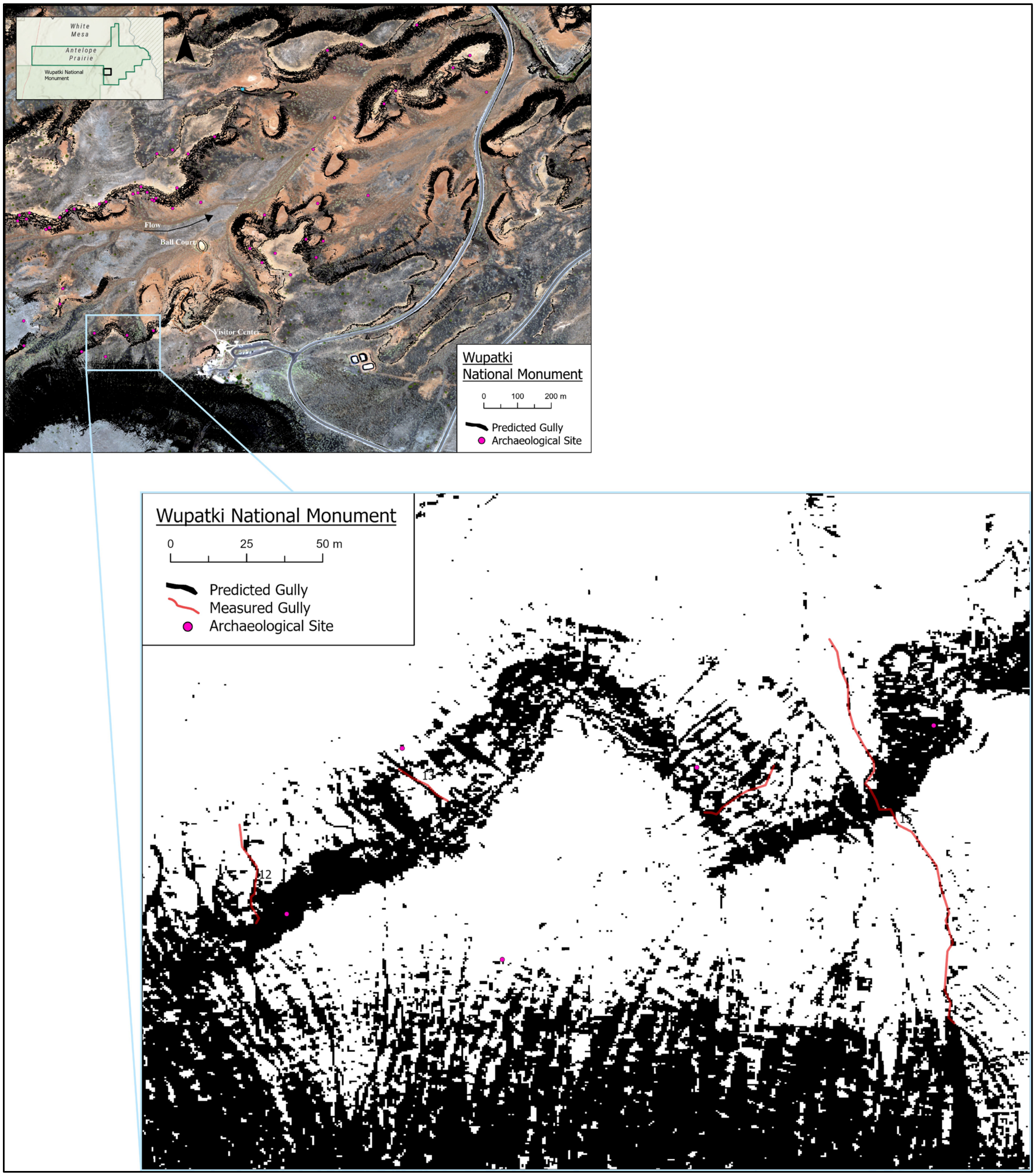

Figure A1. Gully prediction map showing predicted locations of gullies based on the slope-area analysis threshold model. The threshold model overpredicted gully locations and needs to consider additional factors beyond topography such as lithological influences on gully formation.

The Department of the Interior protects and manages the nation's natural resources and cultural heritage; provides scientific and other information about those resources; and honors its special responsibilities to American Indians, Alaska Natives, and affiliated Island Communities.

NPS 322/192780, February 2024

National Park Service
U.S. Department of the Interior

[Natural Resource Stewardship and Science]
1201 Oakridge Drive, Suite 150
Fort Collins, CO 80525

EXPERIENCE YOUR AMERICA ™